JIRRS
Journal International Review of Research Studies

Received: 18/04/ 2026 - **Accepted:** 15/07/2026
Vol: 01.06
DOI: 10.66104/jwmrvy32
Pages: 1-43

When Should Carbon and Aluminum Be Combined as Reductants? A Critical Review and Process-Selection Framework for Hybrid Carbothermic–Aluminothermic Reduction

Antonio Clareti Pereira, PhD
PhD in Chemical Engineering
Federal University of Minas Gerais (UFMG))
Belo Horizonte, Minas Gerais, Brazil
E-mail: claretipereira@gmail.com
ORCID: https://orcid.org/0000-0001-8115-4279

Abstract

Carbothermic and aluminothermic reduction occupy complementary but non-interchangeable roles in metallurgical process design. Carbon is inexpensive, scalable, and compatible with established furnaces, but it generates CO/CO_2, promotes carbon pickup and carbide formation, and may require substantial external heat. Aluminum has a stronger oxygen affinity and releases intense exothermic heat, enabling reduction of stable oxides and production of low-carbon metals, but it increases reductant cost, generates Al_2O_3-rich slag, and raises risks from residual aluminum, aluminides, and inclusions. This critical review examines when combining both reductants is technically, economically, and environmentally justified. The corpus comprises 83 publications, including 81 from 2020–2026 and two earlier studies from 2015–2016 retained as historical evidence on self-reducing nickel agglomerates. Hybrid carbothermic–aluminothermic reduction is defined as deliberate allocation of reducible oxygen between C/CO and Al through simultaneous co-reduction, carbon-based pre-reduction followed by aluminothermic finishing, aluminum-assisted carbothermy, or staged addition within one reactor. Two descriptors are emphasized: φAl, the fraction of removed oxygen assigned to aluminum, and λR, the total reducing-equivalent ratio, distinguishing nominal charge-based values from measured oxygen balances. The review integrates thermodynamics, Boudouard chemistry, kinetics, thermal coupling, carbon activity, carbide formation, slag liquidus and viscosity, metal-droplet coalescence, reactor design, product quality, techno-economics, life-cycle implications, and scale-up. Evidence is strongest for co-reduction and secondary-feed systems; the retained corpus contains no unambiguous pilot-scale demonstration of C/CO pre-reduction followed by Al finishing. Hybridization is favored when carbon removes bulk oxygen economically and limited aluminum addition overcomes thermodynamic, kinetic, thermal, or quality constraints. The author-developed O–T–K–C–S–Q–E framework organizes conceptual feasibility gates for process selection and scale-up; it is not a validated quantitative scoring or technology-readiness tool.

CC BY

JIRRS
Journal International Review of Research Studies

Received: **18**/04/ 2026 - **Accepted:** 15/07/2026
Vol: 01.06
DOI: 10.66104/jwmrvy32
Pages: 1-43

Keywords: aluminothermy; carbothermy; hybrid reduction; metallothermic reduction; slag engineering; decarbonization

Highlights

- Hybrid C–Al reduction should be defined by deliberate oxygen allocation, not merely by the co-presence of two reductants.
- The φAl and λR metrics require explicit oxygen balances and a distinction between nominal and measured values.
- Direct co-reduction evidence is growing, but no unambiguous pilot-scale C/CO → Al sequential demonstration was identified in the retained corpus.
- The O–T–K–C–S–Q–E framework links thermodynamics, kinetics, slag separation, quality, TEA/LCA, and scale-up.

1. Introduction

Carbothermic reduction remains the industrial benchmark for many large-tonnage processes because carbonaceous reductants are inexpensive, compatible with continuous furnace operation, and able to couple direct solid–solid reactions with CO-mediated reduction. Its limitations, however, are intrinsic rather than incidental: carbon generates gaseous products, the Boudouard equilibrium strongly couples temperature to reducing potential, dissolved carbon and carbides can enter product chemistry, and comparatively stable oxides may require temperatures or carbon activities that compromise selectivity. Recent work on chromite, manganese ores, ilmenite, tungsten oxides, silicon-bearing systems, and battery-derived oxides illustrates both the versatility and the constraints of carbon-based reduction (Bao et al., 2026; Carter et al., 2026; Du et al., 2025; Larssen et al., 2021a; Larssen et al., 2021b; Mukono et al., 2022; Nuraeni et al., 2022; Sarkar et al., 2026; Subasinghe & Ratnayake, 2021; Subasinghe & Ratnayake, 2025).

Aluminothermy moves the process into a different thermochemical regime. Aluminum's high oxygen affinity can drive reactions that are difficult for C/CO, and the associated heat release can sustain rapid, high-temperature reaction fronts or assist melting with less external power. This thermodynamic advantage comes at the cost of a more expensive reductant, increased Al_2O_3-bearing slag mass, possible residual Al or aluminide formation, and greater sensitivity to interfacial transport, particle size, ignition, heat loss, and metal–slag separation. These constraints are evident

CC BY

JIRRS
Journal International Review of Research Studies

Received: **18**/04/ 2026 - **Accepted:** 15/07/2026
Vol: 01.06
DOI: 10.66104/jwmrvy32
Pages: 1-43

across Fe_2O_3–Al thermite systems, ferrotitanium, MnO-bearing slags, Al–Zr alloys, CeO_2 reduction, and emerging rare-earth or titanium-alloy production (Amon et al., 2024; Chen et al., 2022; Choi et al., 2020; de Souza & de Lemos, 2021; de Souza et al., 2024; Jiang et al., 2026a; Jiang et al., 2026b; Kudyba et al., 2021; Rhamdani et al., 2026).

The central engineering question, therefore, is not whether carbon or aluminum is the better reductant in the abstract. The useful question is how much oxygen each reductant should remove, in what sequence, at what temperature, and with what consequences for gas generation, slag mass, carbon pickup, inclusion chemistry, metal recovery, and cost. Hybrid reduction requires deliberate process architecture. Aluminum may finish a carbon pre-reduction, be introduced in limited amounts to supply useful heat, act as a terminal deoxidizer after the main metallization step, or be metered in stages so C/CO and Al operate in different oxygen-potential windows. Direct Al–C co-reduction, aluminum-dross-assisted self-reduction, mixed-reductant manganese studies, and direct comparisons of carbothermic and aluminothermic battery-material reduction collectively define this design space, although they do not provide the same level of evidential directness (Coetsee & De Bruin, 2025; Ma et al., 2022; Wiszniewski et al., 2025; Xin et al., 2021).

As summarized in Table 1, hybridization is justified only when it resolves a specific penalty of either parent route. Combining reductants without controlling oxygen allocation, heat release, slag chemistry, residence time, and finishing requirements can simply accumulate the disadvantages of both systems. Conversely, staged oxygen allocation can use low-cost carbon for bulk reduction while reserving aluminum for difficult residual oxygen, product-quality control, or thermal intensification. This criterion—minimum Al use consistent with the required metallurgical outcome—provides the decision logic used throughout the review.

Table 1. *Fundamental comparison of carbothermic, aluminothermic, and hybrid C–Al reduction.*

Criterion	Carbothermic (C)	Hybrid (C + Al)	Aluminothermic (Al)
Reductant cost	Generally low	Intermediate and tunable	Generally high
Direct CO/CO_2 generation	High	Reduced as φAl increases	Very low from reduction itself

CC BY

JIRRS Journal International Review of Research Studies

Received: 18/04/ 2026 - **Accepted:** 15/07/2026
Vol: 01.06
DOI: 10.66104/jwmrvy32
Pages: 1-43

Carbon pickup/carbides	Potentially high	Controllable through carbon share	Low, unless carbon is introduced elsewhere
Chemical heat release	Limited/route-dependent	Potentially synergistic	High
Al_2O_3 slag burden	Low unless feed contains Al	Increases with Al share	Highest
Product flexibility	Best for C-tolerant alloys	Broad design window if controlled	Strong for low-C/high-value products
Scale-up maturity	High	Emerging; feed- and architecture-specific	Established in selected batch/semicontinuous applications

Note. Critical synthesis based on Güney et al. (2023), Holappa and Nurmi (2025), Nababan et al. (2026), Pastor-Vallés et al. (2025), and Zhu et al. (2024).

Figure 1 formalizes the taxonomy used throughout this review. The essential distinction is whether the route is purely carbothermic, purely aluminothermic, or intentionally hybrid through shared oxygen removal. Within the hybrid class, simultaneous addition is only one configuration; sequential and dynamically staged configurations may offer greater control, but their evidence base must be distinguished from process analogs that use a non-carbon pre-reductant.

CC BY

JIRRS
Journal International Review of Research Studies

Received: 18/04/ 2026 - **Accepted:** 15/07/2026
Vol: 01.06
DOI: 10.66104/jwmrvy32
Pages: 1-43

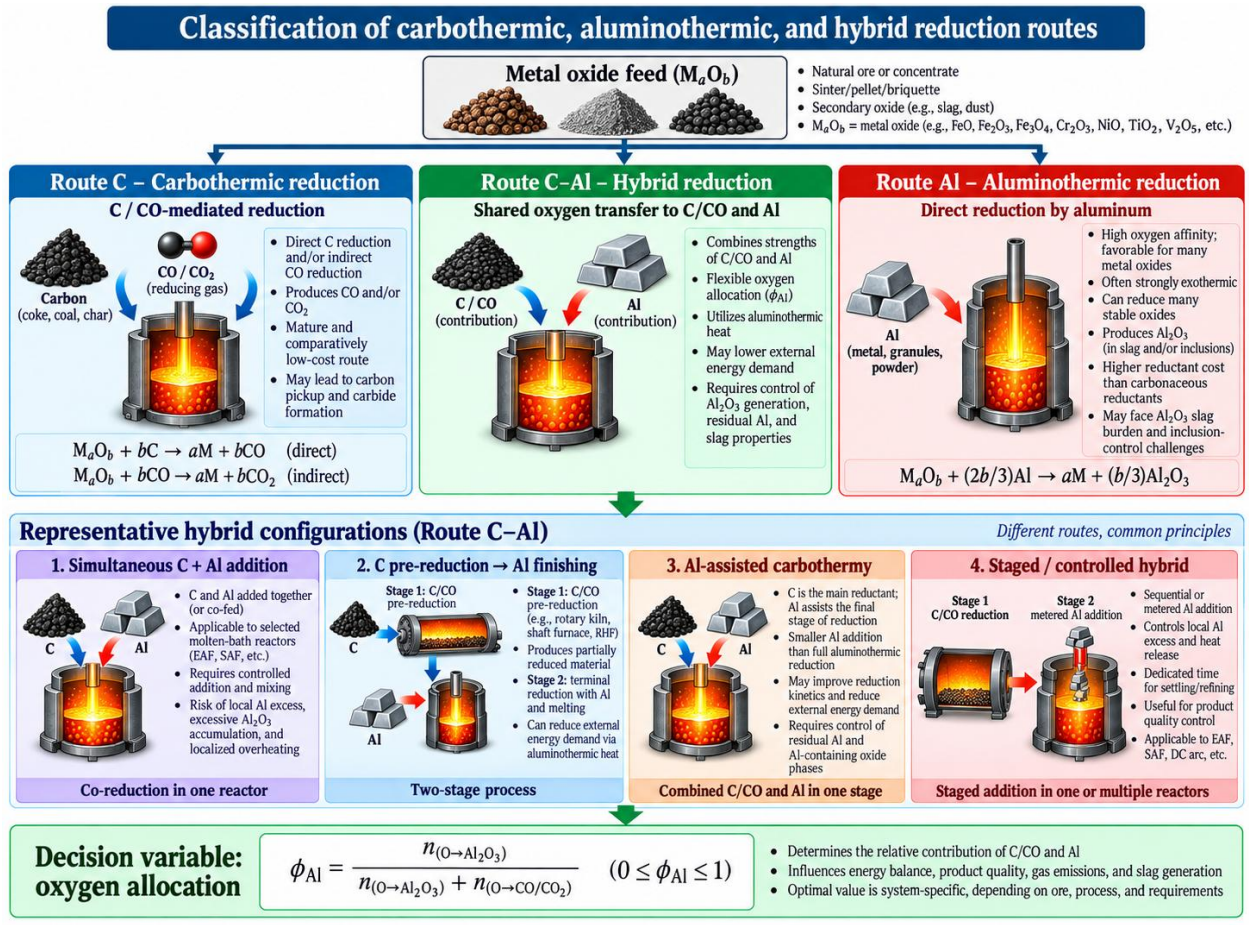

Figure 1. *Classification of carbothermic, aluminothermic, and hybrid reduction routes.*

Note. Original schematic by the author, based on the process concepts reported by Ma et al. (2022), Wiszniewski et al. (2025), Xin et al. (2021), and the scale-relevant staged-process analog of Mchabe et al. (2026).

2. Review Methodology, Scope, and Evidence Classification

2.1 Scope and search logic

This study is positioned as a structured critical review rather than a systematic review or meta-analysis. The analytical corpus contains 83 publications: 81 dated 2020-2026, with two studies from 2015–2016 retained only as historical/contextual evidence on self-reducing and pre-reduced nickel agglomerates. Foundational thermodynamic references cited only to establish classical

CC BY

JIRRS
Journal International Review of Research Studies
Received: **18**/04/ 2026 - **Accepted:** 15/07/2026
Vol: 01.06
DOI: 10.66104/jwmrvy32
Pages: 1-43

principles are treated as background sources and are not counted in the 83-publication analytical corpus. The corpus was organized around the process-selection problem implied by the title rather than around individual metals. The analytical search concepts included carbothermic–aluminothermic reduction, aluminum-assisted carbothermy, carbon–aluminum co-reduction, carbon/CO pre-reduction followed by aluminothermic finishing, thermite kinetics, CO/CO_2 reduction, slag viscosity, metal-droplet settling, reductant allocation, low-carbon alloy production, reactor scale-up, and life-cycle performance. The manuscript does not claim systematic-review completeness; instead, it makes scope and evidential directness explicit so that mechanistic transfer is not confused with direct hybrid validation.

Studies were excluded from the analytical core when they were purely hydrometallurgical, when Al or C was present only as an inert impurity, when the process did not involve reducible oxide/slag chemistry relevant to the review question, or when the information was insufficient to support a process-level or mechanistic inference. Studies were retained as transferable evidence when they clarified oxygen potential, thermal propagation, liquid-Al interfacial reaction, Boudouard control, carbide formation, slag rheology, droplet coalescence, reactor heat loss, product quality, or life-cycle implications relevant to hybrid design. We interpreted each source against four questions: whether C and Al were both active reductants; whether the configuration was simultaneous or sequential; whether the scale and measurements supported process-level inference; and whether the result demonstrated hybrid chemistry directly or provided a transferable mechanism. Only English-language records with sufficient bibliographic and technical information for critical evaluation were retained.

2.2 Evidence classes

Table 2 classifies evidence by directness and transferability rather than by universal scientific quality. Type I evidence uses C and Al as active reductants within one integrated route. Type II denotes the specific sequential architecture of carbon/CO pre-reduction followed by Al finishing; importantly, the retained corpus contains no unambiguous pilot-scale demonstration of this exact C/CO → Al sequence. Type III includes parent-route comparisons and process-architecture

CC BY

JIRRS
Journal International Review of Research Studies

Received: **18**/04/ 2026 - **Accepted:** 15/07/2026
Vol: 01.06
DOI: 10.66104/jwmrvy32
Pages: 1-43

analogs, including hydrogen pre-reduction followed by aluminothermic smelting, which can inform reactor integration without directly validating C–Al. Type IV transfers well-characterized thermodynamic, kinetic, slag, or separation mechanisms from C/CO, Al/Al_2O_3, metal–slag, and thermite systems. These classes therefore describe evidential directness and transferability, not a ranking of study quality.

Table 2. Evidence classes by directness and transferability for hybrid carbothermic–aluminothermic reduction.

Evidence class	Definition	Representative examples	Use in this review
Type I—direct hybrid	C and Al are both active reductants in one integrated route	Al–C reduction roasting; Al-dross + carbon/graphite systems	Direct evidence of coupled C–Al chemistry
Type II—sequential C/CO → Al	Carbon/CO pre-reduction followed by Al finishing	No unambiguous pilot-scale example in the retained corpus	Key evidence gap; target architecture for validation
Type III—comparative/analogue	Parent routes compared on similar feeds, or staged architecture with a non-C pre-reductant	Carbo- vs aluminothermic battery materials; H_2 pre-reduction → Al finishing	Transferable comparative/architecture evidence; does not validate C–Al coupling
Type IV—mechanistic	Transferable thermodynamics, kinetics, slag, or separation evidence	Thermite propagation; CO/CO_2 reduction; droplet settling	Transferable mechanistic evidence; does not constitute direct hybrid validation

Note. Evidence classes synthesized from An et al. (2023), Ma et al. (2022), Mchabe et al. (2026), Mitas et al. (2023), Tichtchenko et al. (2021), Wiszniewski et al. (2025), and Xin et al. (2021).

3. Taxonomy of Hybrid Configurations and Application Space

3.1 Simultaneous, sequential, assisted, and staged modes

A simultaneous hybrid charge contains oxide, carbon, aluminum, and, where required, flux from the start. This architecture maximizes thermal interaction because aluminothermic heat can immediately raise local temperature, accelerate carbon gasification, promote melting, and shorten externally heated stages. The same coupling reduces controllability: reaction fronts may localize, Al can be consumed by oxides that carbon could have reduced more economically, and rapid Al_2O_3

CC BY

JIRRS
Journal International Review of Research Studies
Received: **18**/04/ 2026 - **Accepted:** 15/07/2026
Vol: 01.06
DOI: 10.66104/jwmrvy32
Pages: 1-43

generation can change liquidus and viscosity before metal droplets have coalesced. Thermite models show that conductivity, particle contact, diffusion-limited kinetics, and Al particle size strongly influence front propagation and ignition sensitivity (Abdelal, 2026; Song et al., 2020; Tichtchenko et al., 2021).

Sequential reduction separates bulk oxygen removal from the finishing step. In the target hybrid architecture, carbon or CO first removes a large fraction of oxygen, after which Al performs final reduction, deoxidation, or alloy formation. No unambiguous pilot-scale demonstration of this exact C/CO → Al sequence was identified in the retained corpus. Mchabe et al. (2026) instead provide a scale-relevant architecture analog: hydrogen-pre-reduced manganese ores were subsequently treated by aluminothermic smelting in a 200 kW direct-current (DC) arc furnace. That study demonstrates the engineering feasibility of separating pre-reduction from aluminothermic finishing, but it should not be counted as direct evidence of carbothermic–aluminothermic coupling. The sequential concept therefore remains metallurgically plausible and industrially attractive, but it requires direct C/CO-based pilot validation.

Al-assisted carbothermy uses less Al than stoichiometric aluminothermy. In this configuration, Al functions as a thermochemical intensifier and partial oxygen sink rather than as the sole reductant: its reaction heat may accelerate Boudouard gasification, promote local melting, and shorten the time required for carbon-based oxygen removal. A related strategy uses Al-bearing secondary materials, especially aluminum dross, as both reductant and heat source, turning a secondary stream into an active process reagent (Wongsawan et al., 2022; Xin et al., 2021). Staged addition extends this logic by metering Al only after off-gas, temperature, or metal chemistry indicates that carbon has completed the low-cost portion of reduction.

3.2 Feedstocks and products

Hybridization is most relevant where the parent routes have complementary limitations, but the strength of evidence varies by system. Chromium systems face carbon pickup and carbide formation under strongly carbothermic conditions, whereas low-carbon ferrochrome requires tighter control of terminal oxygen removal (Carter et al., 2026; Güney et al., 2023). Manganese is

CC BY

JIRRS
Journal International Review of Research Studies

Received: **18**/04/ 2026 - **Accepted:** 15/07/2026
Vol: 01.06
DOI: 10.66104/jwmrvy32
Pages: 1-43

a strong candidate for staged processing because CO/CO_2 pre-reduction is well characterized and aluminothermic finishing can target ultra-low-carbon FeMn; however, the exact C/CO → Al sequence still lacks direct pilot-scale validation in the retained corpus (Kumar et al., 2026; Larssen et al., 2021a; Larssen et al., 2021b; Larssen & Tangstad, 2022). Titanium systems expose the opposite contamination problem: carbon can promote TiC formation, while aluminum can enter Ti-bearing alloys and generate large aluminous-slag burdens (Choi et al., 2020; Yang et al., 2022; You et al., 2024).

Silicon provides an important decarbonization boundary case. Conventional production relies on high-temperature carbothermy, whereas recent aluminothermic work has progressed from thermodynamic studies to pilot-scale production and life-cycle assessment. Aluminothermy can reduce direct carbon-derived emissions, but its system-level benefit depends strongly on the carbon intensity and circularity of the aluminum supply (Hoover et al., 2024; Pastor-Vallés et al., 2025; Zhu et al., 2024). Ni/Co-bearing laterites, slags, and battery materials provide a second application space because carbon reduction, metal collection, and aluminum-bearing components can interact in complex ways; here, phase partitioning and impurity transfer are as important as nominal reduction degree (Hu et al., 2025; Klemettinen et al., 2024; Nuraeni et al., 2022; Sarkar et al., 2026).

Table 3 maps representative feed classes to the process bottleneck that hybridization is intended to address. The table emphasizes the constraint rather than the metal because similar process logic can transfer across feedstocks, but transferability should be treated as a hypothesis until demonstrated directly.

Table 3. *Feedstock classes and the process rationale for hybrid C–Al reduction.*

Feed/product class	Carbothermic constraint	Potential role of Al	Key hybrid risk
Cr oxides/chromite	Carbide and high-C alloy formation	Low-C finishing; heat release	Al_2O_3-rich slag; Al cost
Mn ores/slags	Well-characterized C/CO pre-reduction; final C control	Potential ultra-low-C finishing; sequential route still under-validated	Inclusions; slag separation

CC BY

JIRRS
Journal International Review of Research Studies

Received: **18**/04/ 2026 - **Accepted:** 15/07/2026
Vol: 01.06
DOI: 10.66104/jwmrvy32
Pages: 1-43

Feed/product class	Carbothermic constraint	Potential role of Al	Key hybrid risk
Ti feeds	TiC tendency and high temperature	Strong reduction and alloying	Residual Al; aluminous slag
V/Nb/Mo/W oxides	Difficult final oxygen removal	Selective final reduction	Excess heat; alloy contamination
Silica/silicate slags	Very high carbothermic temperature	Lower direct-C route and potential finishing heat	Embedded emissions of Al
Secondary/battery feeds	Complex multi-oxide reduction	Direct co-reduction, partitioning, and/or collector formation	Impurity redistribution

Note. Representative evidence from Bao et al. (2026), Güney et al. (2023), Kumar et al. (2026), Makhambetov et al. (2026), Mchabe et al. (2026), Nababan et al. (2024a, 2024b), Sheybani et al. (2020), Wang et al. (2025), and Zhu et al. (2024).

4. Thermodynamic Basis and Quantitative Oxygen Allocation

4.1 Carbon, CO/CO_2, and the Boudouard constraint

The thermodynamic role of carbon cannot be represented by a single reaction such as $MO + C \rightarrow M + CO$. In many porous or agglomerated systems, solid carbon first controls the CO/CO_2 ratio through the Boudouard equilibrium, $C + CO_2 \rightleftharpoons 2CO$, and CO subsequently reduces the oxide. Temperature therefore affects both oxide equilibrium and the availability of CO. Detailed studies of manganese ores and calcium ferrite confirm that reduction rate and degree depend on gas composition, reaction sequence, porosity, and evolving mineral structure (An et al., 2023; Larssen et al., 2021a; Larssen et al., 2021b; Mukono et al., 2022; Panteikov et al., 2024). In practice, the reducing potential of a carbon stage is better described by oxygen potential and gas ratio than by kilograms of fixed carbon alone.

4.2 Aluminum as a terminal oxygen sink

Classical oxygen-potential analysis provides the thermodynamic baseline for comparing reductants (Ellingham, 1944). Aluminothermy is governed by the high thermodynamic stability of Al_2O_3, but real processes deviate from ideal Ellingham comparisons because activities, intermediate oxides, slag dissolution, interfacial films, and alloy formation modify the effective driving force. Studies of Al–Zr, $TiO_2/CaTiO_3$, Mn oxides, and Mo/V oxides show that reaction

CC BY

JIRRS
Journal International Review of Research Studies
Received: **18**/04/ 2026 - **Accepted:** 15/07/2026
Vol: 01.06
DOI: 10.66104/jwmrvy32
Pages: 1-43

pathways depend on fluxes, metal collectors, phase formation, and the ability of the slag to dissolve Al_2O_3 and residual oxides (Cai et al., 2026; Chen et al., 2022; Salas Avilés et al., 2023; Wang et al., 2025; Yang et al., 2022). The useful hybrid question is therefore not whether Al can reduce a difficult oxide, but at what residual oxygen level carbon-based removal becomes disproportionately slow, energy-intensive, contamination-prone, or expensive.

4.3 Hybridization parameter and reductant sufficiency

Two related quantities are needed to compare hybrid systems, but you must first define the target product specification because allowable C, O, Al, carbide, aluminide, and inclusion levels constrain the feasible oxygen-allocation window. First, oxygen allocation is defined on an oxygen-atom basis as $\varphi C = nO,C/nO,removed$ and $\varphi Al = nO,Al/nO,removed$, with $\varphi C + \varphi Al = 1$. Here, nO,C is the oxygen transferred to net carbon-derived products, principally CO and CO_2, and nO,Al is the oxygen fixed in Al-containing reduction products attributable to oxygen transfer, principally Al_2O_3. Pure carbothermy corresponds to $\varphi Al = 0$, pure aluminothermy to $\varphi Al = 1$, and an intentionally hybrid process to $0 < \varphi Al < 1$. φAl is therefore an oxygen-allocation fraction, not the fraction of total charged reductant mass represented by Al. For experiments, reconstruct balance-derived values from off-gas, slag, and metal analyses. Aluminum retained as dissolved Al, aluminides, residual metallic Al, or other non-oxygen-transfer phases is excluded from nO,Al; Al consumed by gangue contributes only to the extent that a demonstrable oxygen transfer from reducible gangue oxide to an Al-bearing oxidation product is included in the declared process oxygen balance. Residual carbon and carbide-bound carbon are likewise not counted as oxygen transferred to carbon-derived gas products.

Second, the total reducing-equivalent ratio is defined as $\lambda R = (nO,cap,C + nO,cap,Al)/nO,reducible$. λR must be calculated from chemically available reducing equivalents rather than gross reductant mass. For pure Al terminating as Al_2O_3, the nominal oxygen capacity is 1.5 mol O per mol reactive Al; for aluminum dross or low-grade scrap, only the measured or otherwise justified reactive metallic-Al fraction should be credited. For carbonaceous reductants, fixed/reactive carbon must be distinguished from ash, volatiles, moisture, and non-reactive mineral

CC BY

JIRRS
Journal International Review of Research Studies

Received: **18**/04/ 2026 - **Accepted:** 15/07/2026
Vol: 01.06
DOI: 10.66104/jwmrvy32
Pages: 1-43

matter. For carbon discharged as a net CO/CO_2 mixture, the effective oxygen capacity depends on the declared gas endpoint; if $yCO_2 = nCO_2/(nCO + nCO_2)$, one mole of reacted carbon carries $(1 + yCO_2)$ mol O. Values of λR below unity indicate reductant deficiency, values near unity describe nominal stoichiometry, and values above unity quantify global excess. Reporting both allocation (φAl, φC) and sufficiency (λR), together with whether values are nominal or balance-derived, prevents experiments with very different gas generation, slag mass, and product carbon from being treated as equivalent.

Worked oxygen-balance example. Consider a feed from which 100 mol of reducible oxygen is removed. Suppose the measured dry off-gas contains 30 mol CO and 20 mol CO_2; the oxygen transferred to carbon-derived gas is then $nO,C = 30 + 2(20) = 70$ mol O. If slag analysis and phase accounting show that 10 mol Al_2O_3 were generated by reductive oxygen transfer, $nO,Al = 30$ mol O and $\varphi Al = 30/100 = 0.30$ ($\varphi C = 0.70$). If 25 mol Al were charged but only 20 mol entered Al_2O_3, with 3 mol dissolved/alloyed and 2 mol residual metallic Al, only the 20 mol reductively oxidized Al are used to reconstruct φAl. For a separate nominal sufficiency calculation, if 60 mol of chemically available C are supplied with an assumed gas endpoint $yCO_2 = 0.40$ and 25 mol of reactive Al are available, the nominal capacities are 84 and 37.5 mol O, respectively, giving $\lambda R = (84 + 37.5)/100 = 1.215$. The example illustrates why φAl (actual oxygen allocation) and λR (supplied reducing capacity) are distinct quantities.

Figure 2 visualizes a representative staged/sequential thermodynamic trajectory in which carbon/CO removes oxygen where reduction is kinetically accessible and economically favorable, and Al is reserved for a residual oxygen-potential window in which carbon becomes rate-, energy-, or quality-limiting. The transition is feed-specific and moves with temperature, activities, slag composition, carbon activity, and product specification. Simultaneous co-reduction need not follow this clean sequence or a monotonic oxygen-potential history, so interpret the figure as one process architecture rather than a universal trajectory for all C–Al hybrid systems.

CC BY

JIRRS
Journal International Review of Research Studies

Received: **18**/04/ 2026 - **Accepted:** 15/07/2026
Vol: 01.06
DOI: 10.66104/jwmrvy32
Pages: 1-43

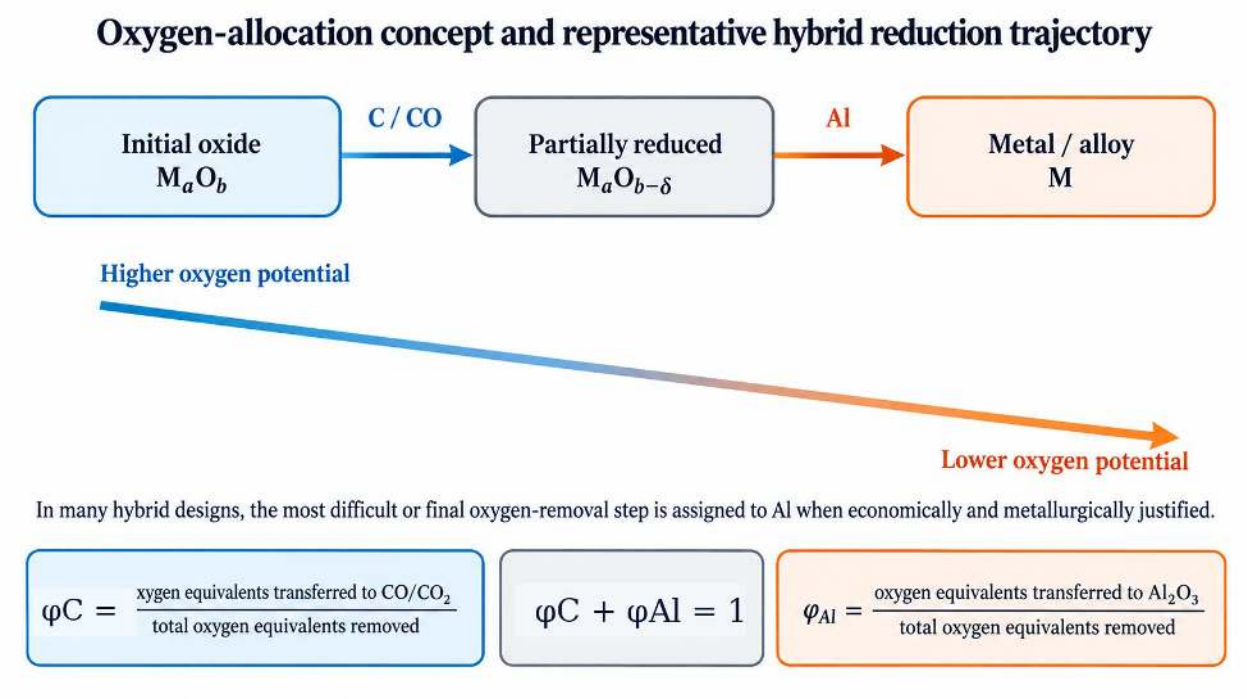

Figure 2. Oxygen-allocation concept and representative staged/sequential reduction trajectory in a hybrid system.

Note. Original process-design schematic by the author, based on CO/CO_2 reduction and aluminothermic thermodynamic evidence reported by An et al. (2023), Chen et al. (2022), Kudyba et al. (2021), Larssen et al. (2021a, 2021b), and Nababan et al. (2026).

Table 4 summarizes the thermodynamic and operational variables that determine where to place the C/CO-to-Al transition. It also shows why an Ellingham-only comparison is insufficient: the practical boundary depends on activities, phase state, gas composition, slag transport, and product constraints.

Table 4. *Variables controlling the optimum oxygen allocation between C/CO and Al.*

Variable	Effect on carbon stage	Effect on Al stage	Hybrid implication
Temperature	Raises Boudouard activity and diffusion	Changes liquid-Al transport and slag fluidity	Shifts optimal transition point

CC BY

JIRRS Journal International Review of Research Studies

Received: **18**/04/ 2026 - **Accepted:** 15/07/2026
Vol: 01.06
DOI: 10.66104/jwmrvy32
Pages: 1-43

Variable	Effect on carbon stage	Effect on Al stage	Hybrid implication
pO_2 / CO/(CO + CO_2)	Directly controls gas reduction potential	Sets residual oxygen demand	Potential state indicator for staged Al addition; requires reactor-specific calibration with temperature and metal/slag chemistry
Carbon activity	Controls carburization/carbides	Indirect	May justify earlier transfer to Al
Oxide activity in slag	Can slow final C reduction	Changes Al requirement and yield	Requires activity-based, not pure-oxide, calculations
Al_2O_3 activity/solubility	Minor in C-only stage	Controls product layer/slag chemistry	Flux design becomes part of reductant design
Metal activity/alloying	Can stabilize carbides	Can stabilize aluminides/intermetallics	Product specification determines allowable φAl

Note. Synthesized from Feng et al. (2020), Holappa and Nurmi (2025), Philipson et al. (2024b), Sun et al. (2024), and Xin et al. (2022).

5. Thermal Coupling, Reaction Mechanisms, and Kinetics

5.1 Coupled mechanisms

Hybrid systems combine at least three kinetic pathways: direct or contact-mediated solid-carbon reduction, gas-mediated CO reduction, and aluminum-mediated interfacial reduction. When Al melts, wetting and liquid–liquid or liquid–solid transport can rapidly change the effective reaction area. Experimental work on aluminum reacting with calcium-silicate slags shows that droplet deformation, interfacial renewal, and product-layer behavior can become rate-controlling (Philipson et al., 2024a; Philipson et al., 2024b). In parallel, thermite studies show that thermal conductivity, contact resistance, diffusion, and particle size control propagation velocity (Abdelal, 2026; de Souza & de Lemos, 2021; de Souza et al., 2024; Song et al., 2020; Tichtchenko et al., 2021).

Coupling can be synergistic, additive, or antagonistic. Synergy occurs when Al-derived heat increases carbon gasification, accelerates melting, breaks diffusion barriers, or promotes metal coalescence. Additivity occurs when the two reductants operate in largely separate domains. Antagonism occurs when rapidly formed Al_2O_3 or spinel-rich material coats reacting surfaces, increases slag viscosity, immobilizes droplets, or diverts Al toward low-value oxides. Figure 3

CC BY

JIRRS
Journal International Review of Research Studies

Received: 18/04/ 2026 - **Accepted:** 15/07/2026
Vol: 01.06
DOI: 10.66104/jwmrvy32
Pages: 1-43

separates these regimes explicitly so that "hybrid" is not automatically interpreted as "synergistic." A claim of synergy should therefore be supported by appropriate single-reductant controls and, where possible, a factorial C × Al design at matched temperature, residence time, and total reducing capacity so that thermal, chemical, and mixing effects are not confounded.

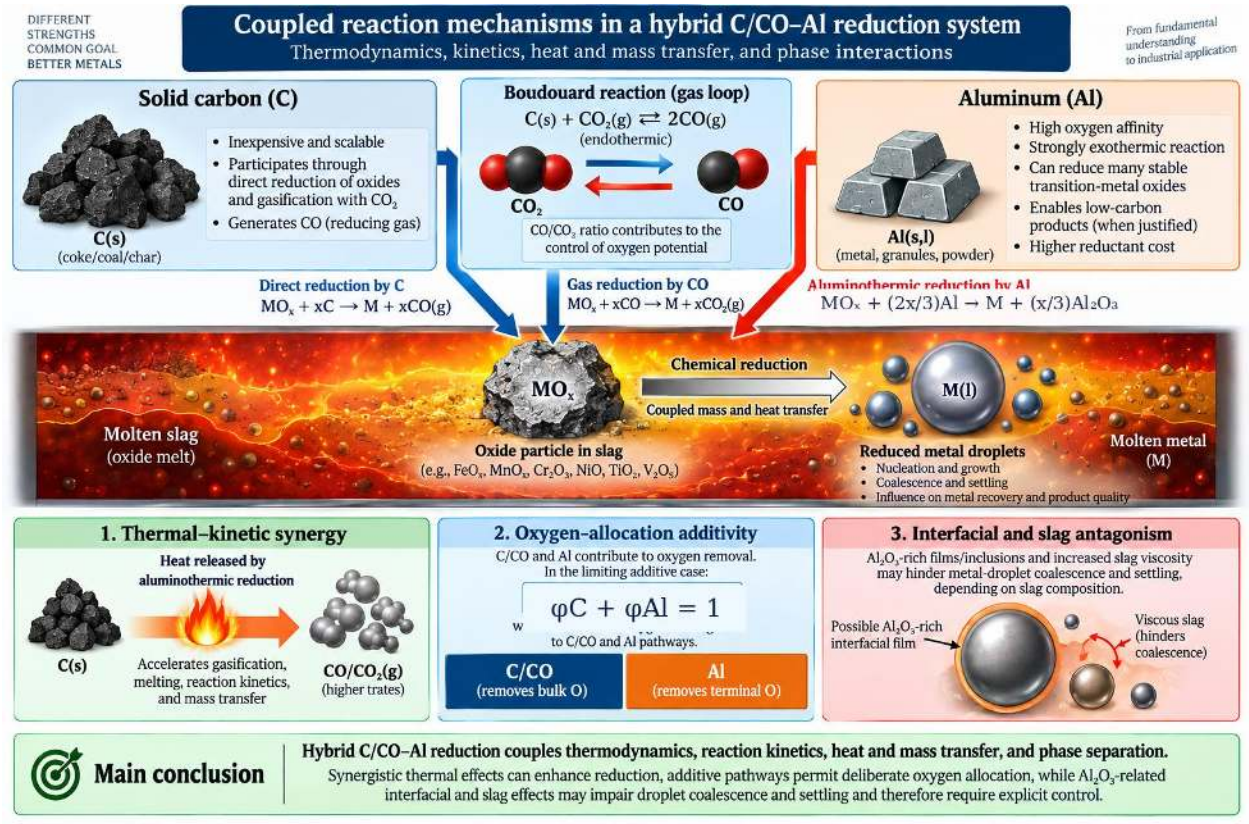

Figure 3. *Coupled reaction mechanisms and possible interaction regimes in a hybrid C–Al system.*
Note. Original schematic by the author, based on thermite-propagation, liquid-Al/slag, and gas-reduction evidence from de Souza and de Lemos (2021), de Souza et al. (2024), Philipson et al. (2024a, 2024b), and Tichtchenko et al. (2021).

5.2 Heat balance and useful aluminothermic heat

For a defined batch or mass basis, the hybrid energy balance can be expressed conceptually as Qext + Qfeed + Qrxn,Al = Qred + Qmelt + Qgas + Qloss, where Qext is external heat or electrical power input, Qfeed is sensible heat supplied with hot feed or pre-reduced material, Qrxn,Al is the net heat released by aluminothermic reduction, Qred is the heat required for oxide reduction

CC BY

JIRRS
Journal International Review of Research Studies

Received: 18/04/ 2026 - **Accepted:** 15/07/2026
Vol: 01.06
DOI: 10.66104/jwmrvy32
Pages: 1-43

through the C/CO pathway, Qmelt includes melting and slag-formation duties, Qgas represents off-gas sensible heat and endothermic CO generation, and Qloss represents heat losses through the vessel, refractory, and openings. All terms must be reported on the same basis and with a declared sign convention. The critical quantity is not gross aluminothermic heat release, but the fraction captured as avoided external energy, accelerated carbon-based reduction, melting, or effective metal–slag separation rather than lost to refractory, off-gas, or localized overheating. In vessel-scale aluminothermy, preheating and wall losses materially change charge temperature and reaction stability (Semenov et al., 2024). In silicon pilot work, heat management and slag formation are equally important because metal production is accompanied by large oxide-to-slag conversions (Zhu et al., 2024).

Adiabatic temperature is therefore useful as a screening index but should not be treated as a scale-up criterion. Continuous electric furnaces, staged feeds, and hot pre-reduced materials can operate far from a closed adiabatic batch. A practical thermal-synergy measure should compare captured aluminothermic heat with the external energy actually avoided, while also checking whether localized overheating increases refractory wear or metal loss. Figure 4 expresses this logic as an energy-flow problem rather than as a single adiabatic-temperature value. For reporting, a conceptual useful-heat utilization factor may be defined as $\eta_{Al,heat}$ = (external energy avoided or useful process duty attributable to Al)/(net aluminothermic heat released). The numerator must be based on a declared counterfactual or matched reference process, and the metric should not equate gross reaction heat with actual avoided electrical or fuel demand.

CC BY

JIRRS
Journal International Review of Research Studies

Received: 18/04/ 2026 - **Accepted:** 15/07/2026
Vol: 01.06
DOI: 10.66104/jwmrvy32
Pages: 1-43

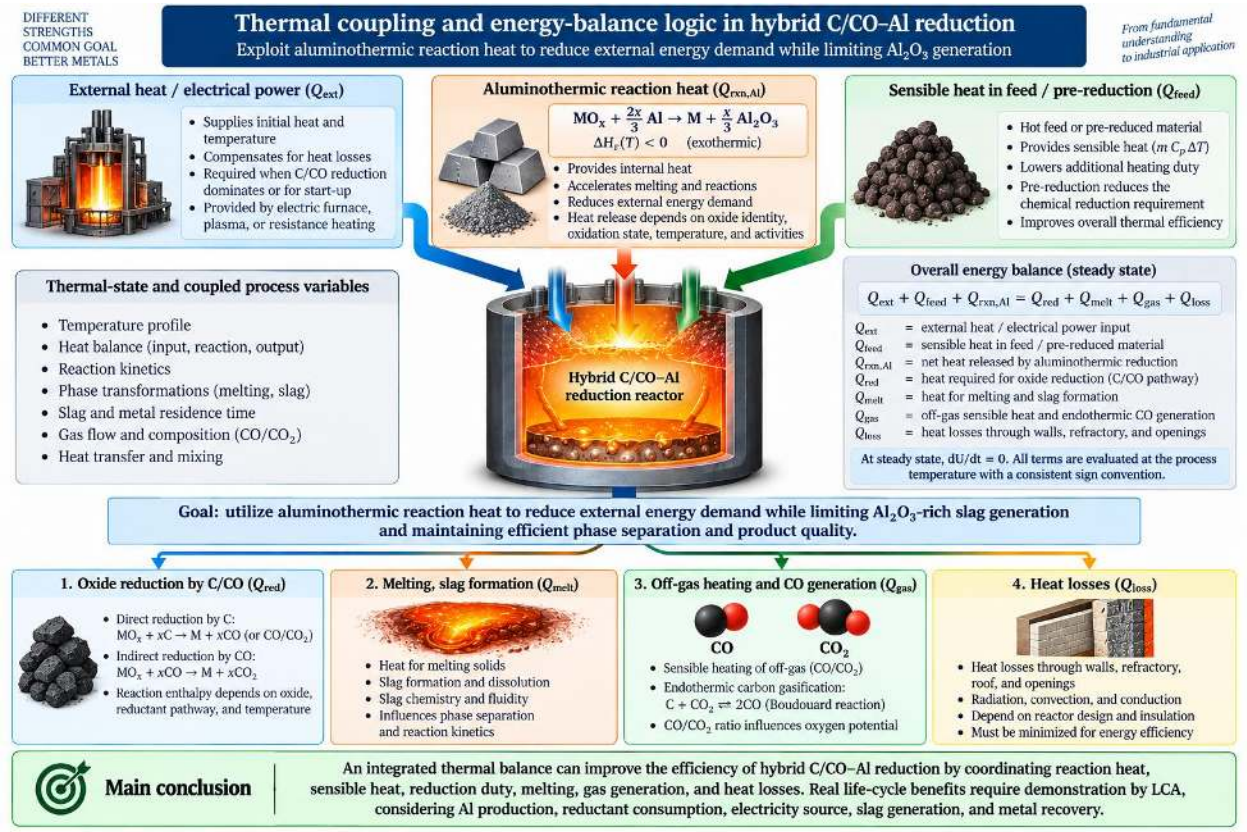

Figure 4. *Thermal coupling and energy-balance logic for hybrid reduction.*

Note. Original schematic by the author, based on reactor-heating models, thermite heat-transfer studies, and pilot aluminothermy reported by de Souza et al. (2024), Semenov et al. (2024), and Zhu et al. (2024).

5.3 Rate-limiting steps and diagnostic observables

Rate control can migrate during a batch: interfacial chemical reaction may dominate initially, pore diffusion or Boudouard gasification during intermediate conversion, and slag-phase mass transfer after melting. The same system can therefore respond differently to carbon reactivity, Al particle size, pellet porosity, mixing, and temperature as conversion proceeds. Microwave and multiphysics studies illustrate how external fields and local heat generation can change apparent kinetics by altering the thermal field rather than intrinsic reaction kinetics alone (Sheybani et al., 2020; Xiong et al., 2025). For scale-up, time-resolved off-gas CO/CO_2, temperature, electrical

CC BY

JIRRS
Journal International Review of Research Studies

Received: 18/04/ 2026 - **Accepted:** 15/07/2026
Vol: 01.06
DOI: 10.66104/jwmrvy32
Pages: 1-43

power, slag composition, and metal chemistry are more informative than final recovery alone because they can identify when the rate-controlling mechanism changes.

6. Carbon Control, Carbides, Residual Aluminum, and Product Quality

One of the strongest rationales for hybridization is control of product chemistry. Increasing the fraction of oxygen removed through carbon can increase carbon dissolution and stabilize carbides such as Cr_7C_3/Cr_3C_2, TiC, VC, WC, and Fe_3C. The tendency depends on carbon activity, temperature, alloy composition, and residence time; total carbon addition is only an imperfect proxy. Chromite reduction, Ti-bearing systems, and carbide-forming tungsten or silicon systems show that a carbon route can generate phases that are difficult or costly to reverse in final refining (Bao et al., 2026; Carter et al., 2026; Subasinghe & Ratnayake, 2021; Subasinghe & Ratnayake, 2025; Sun et al., 2020).

Replacing some carbon with aluminum can reduce carbon exposure, but it introduces a different contamination axis. Residual Al, aluminides, and oxide inclusions can become product-quality constraints. Ultra-low-carbon ferromanganese produced by aluminothermic finishing illustrates the point: achieving low C does not end the quality problem because inclusion population and residual deoxidation products must also be controlled (Kumar et al., 2026). Similar issues arise in Ti–Al–Nb and γ-TiAl systems, where Al is simultaneously a reductant and an alloying element (Jiang et al., 2026a; Jiang et al., 2026b).

Figure 5 shows hybridization as a multi-objective trade-off, not a simple improvement. As φAl rises, carbon pickup, carbide tendency, and net CO/CO_2 decline, while residual-Al risk and Al_2O_3 slag burden increase. These curves are conceptual, not definitive, and the shaded crossing indicates a potential operating window for feed-specific tests.

CC BY

JIRRS
Journal International Review of Research Studies

Received: 18/04/ 2026 - **Accepted:** 15/07/2026
Vol: 01.06
DOI: 10.66104/jwmrvy32
Pages: 1-43

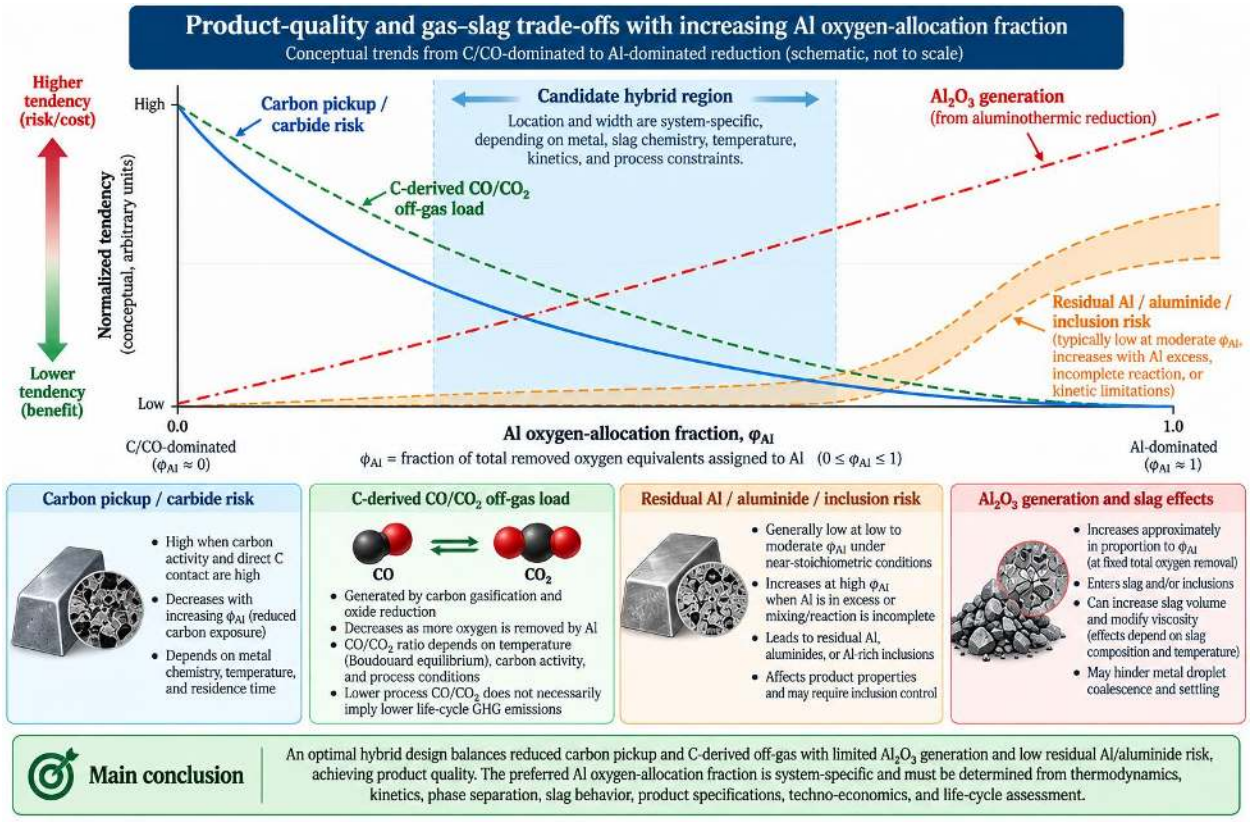

Figure 5. *Conceptual product-quality and gas–slag trade-offs with increasing aluminum share.*

Note. Conceptual synthesis based on low-carbon alloy, slag, and thermochemical evidence from Güney et al. (2023), Kumar et al. (2026), Mchabe et al. (2026), and Wang et al. (2025).

Table 5 translates this trade-off into measurable product-quality variables. A hybrid route should be judged against a predefined specification window for metal chemistry, inclusions, and physical recovery rather than against metallization or chemical reduction alone.

Table 5. *Product-quality variables that should constrain the hybrid operating window.*

Quality variable	Carbothermic risk	Aluminothermic risk	Recommended control metric
Carbon	Dissolution and high-C alloy	Low	wt.% C in metal; carbon activity
Carbides	Cr/Ti/V/W/Fe carbides	Usually low	Phase fraction by XRD and SEM–EDS
Residual Al	Low	Dissolved Al or aluminides	wt.% Al; phase identification

CC BY

JIRRS
Journal International Review of Research Studies

Received: **18**/04/ 2026 - **Accepted:** 15/07/2026
Vol: 01.06
DOI: 10.66104/jwmrvy32
Pages: 1-43

Quality variable	Carbothermic risk	Aluminothermic risk	Recommended control metric
Oxygen/inclusions	Residual oxide; reoxidation	Al_2O_3/spinel inclusions	Total O; inclusion size/chemistry
Si, S, P, and gangue elements	Partition with slag/metal chemistry	Can shift with aluminous slag	Elemental partition ratios
Metallic entrainment	Droplet loss in viscous slag	Can increase with Al_2O_3	Metal in slag; droplet-size distribution

Note. Representative evidence from Kumar et al. (2026), Lyu et al. (2026), Su et al. (2024), and Wang et al. (2024). XRD = X-ray diffraction; SEM–EDS = scanning electron microscopy with energy-dispersive X-ray spectroscopy.

7. Slag Engineering, Gas Generation, and Metal–Slag Separation

7.1 The gas–slag exchange

Carbon and aluminum remove oxygen into fundamentally different product phases. Carbon produces CO/CO_2 gas, whereas aluminum transfers oxygen predominantly into condensed Al_2O_3-bearing phases. Increasing φAl therefore exchanges part of the gas burden for a condensed-slag burden. This shift can reduce off-gas volume and direct carbon-derived emissions, but it increases slag mass, alumina activity, and the need for fluxing and separation. The net effect is composition-specific because added Al_2O_3 can either lower or raise liquidus temperature and viscosity in a multicomponent slag (Coetsee & De Bruin, 2026; Feng et al., 2020).

7.2 Viscosity, coalescence, and settling

Chemical reduction and physical metal recovery are not equivalent. Reduced droplets can remain entrained when slag viscosity is high, density contrast is small, wetting is unfavorable, or available residence time is insufficient. Studies of metal droplets in converter and synthetic slags show that coalescence and settling depend strongly on hydrodynamics, droplet size, and slag properties (He et al., 2020; Lai et al., 2026; Mitas et al., 2023). In aluminothermic systems, in situ slagging has been used deliberately to improve metal–slag separation, confirming that slag design and reduction chemistry must be optimized together (Cheng et al., 2024; Wang et al., 2024).

For approximately spherical droplets settling at low Reynolds number, the Stokes relation is $v_t = g\, d^2(\rho_m - \rho_s)/(18\, \mu_s)$, where v_t is terminal velocity, d is droplet diameter, ρ_m and ρ_s are metal and

CC BY

JIRRS
Journal International Review of Research Studies

Received: **18**/04/ 2026 - **Accepted:** 15/07/2026
Vol: 01.06
DOI: 10.66104/jwmrvy32
Pages: 1-43

slag densities, respectively, and μs is slag viscosity. The d^2 dependence illustrates the severe penalty imposed by fine droplets and viscous slag. Real metallurgical slags depart from the ideal assumptions because coalescence, turbulence, non-spherical droplets, interfacial tension, reaction-driven Marangoni flow, and evolving droplet composition alter settling behavior. The equation should therefore be used as a first-order scale-up diagnostic, not as a complete recovery model.

Table 6 summarizes the principal slag and separation variables that should accompany any report of hybrid reduction. Without these measurements, apparent "reductant synergy" can be confounded by changes in physical separation rather than by a genuine improvement in chemical reduction.

Table 6. *Slag and metal–slag separation variables required to interpret hybrid reduction.*

Variable	Why it matters	Failure mode if uncontrolled	Typical response
Al_2O_3 fraction/activity	Changes network structure and liquidus	High viscosity or refractory solids	Adjust CaO/SiO_2/MgO and flux package
Liquidus temperature	Determines fully liquid residence window	Premature freezing; entrainment	Increase superheat or modify slag
Viscosity	Controls settling/coalescence	Metal trapped in slag	Fluxing, temperature, residence time
Interfacial tension/wetting	Controls droplet attachment and coalescence	Stable dispersed droplets	Modify chemistry and stirring
Droplet size distribution	Strong d^2 effect on settling	Slow recovery despite full reduction	Promote coalescence; limit excessive shear
Residual reducible oxides	Measures chemical loss	Under-reduction misidentified as entrainment loss	Increase reducing capacity or residence time

Note. Synthesized from Feng et al. (2020), He et al. (2020), Lai et al. (2026), Mitas et al. (2023), and Pereira (2026a).

8. Reactor Engineering, Process Integration, and Control

The preferred reactor depends on hybrid architecture. Simultaneous processes can be implemented in an electric arc furnace (EAF), submerged arc furnace (SAF), direct-current (DC) arc furnace, induction furnace, or crucible system, but they require tight control of Al addition rate and thermal transients. Sequential routes can separate a kiln, shaft furnace, rotary-hearth furnace (RHF), fluidized-bed, or electric pre-reduction stage from a second furnace or thermite vessel. The

CC BY

JIRRS
Journal International Review of Research Studies

Received: 18/04/ 2026 - **Accepted:** 15/07/2026
Vol: 01.06
DOI: 10.66104/jwmrvy32
Pages: 1-43

principal engineering advantage of a two-stage route is controllability: carbon-based reduction and aluminothermic finishing can be optimized at different temperatures, gas atmospheres, and residence times. The disadvantages are additional capital expenditure, solids handling, and heat loss during transfer.

Figure 6 compares three reactor configurations. The staged-addition-in-one-furnace concept is especially relevant to retrofit scenarios because it retains one vessel while using off-gas composition and bath temperature as triggers for Al addition. It also avoids transferring partially reduced hot solids. Its feasibility, however, depends on responsive feeding hardware, adequate bath mixing, and safeguards against localized thermal runaway, splashing, and excessive refractory loading.

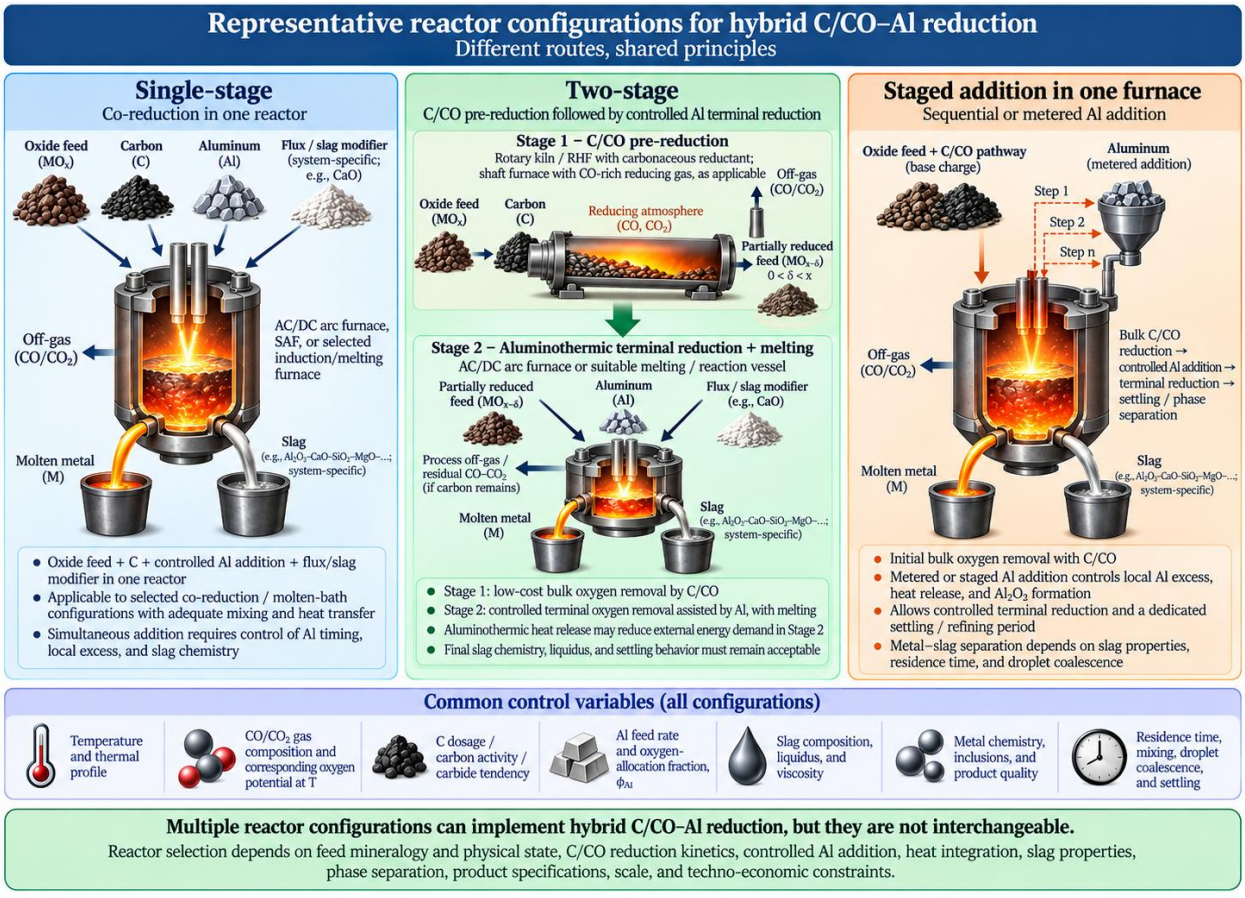

CC BY

JIRRS
Journal International Review of Research Studies

Received: **18**/04/ 2026 - **Accepted:** 15/07/2026
Vol: 01.06
DOI: 10.66104/jwmrvy32
Pages: 1-43

Figure 6. *Representative single-stage, two-stage, and staged-addition reactor configurations.*

Note. Original schematic by the author, based on DC-furnace manganese work, induction-furnace modeling, and pilot aluminothermy reported by Bermúdez et al. (2025), Makhambetov et al. (2026), Mchabe et al. (2026), and Zhu et al. (2024).

Feed preparation is equally important. Carbon reactivity, fixed-carbon content, ash, particle size, Al particle size and purity, mixing, briquetting, pellet porosity, and moisture affect both kinetics and thermal stability. Earlier work on self-reducing and pre-reduced nickel-concentrate agglomerates demonstrated that agglomerate preparation and mechanical performance are integral to downstream thermal processing, providing historical context for current feed-engineering requirements (Feldhagen et al., 2016; Souza et al., 2015). More recent agglomeration studies show that porosity controls gas access and mechanical integrity, while reduction studies on ores and battery materials show that phase evolution can change pore networks during heating (Marmolejo-Saucedo et al., 2024; Nuraeni et al., 2022; Siame et al., 2026). For process control, $CO/(CO + CO_2)$ is a useful indicator of the carbon-reduction regime, while metal chemistry, slag chemistry, and temperature indicate whether the process has entered the finishing window.

Table 7 links reactor choice to the principal scale-up risk. It also emphasizes a fundamental integration problem: batch or rapidly propagating aluminothermy and continuous carbothermy can operate on different process rhythms, so a hybrid flowsheet must reconcile feed, heat-release, and residence-time timescales rather than merely combine unit operations.

Table 7. *Reactor configurations, control variables, and principal scale-up risks.*

Configuration	Strength	Key control variables	Primary scale-up risk
Single-stage simultaneous	Maximum heat coupling; simple flowsheet	Al feed, mixing, temperature, off-gas	Thermal runaway/local over-reduction
Two-stage C/CO → Al	Independent stage optimization; no unambiguous direct pilot-scale demonstration identified in the retained corpus	Pre-reduction degree, hot transfer, Al stoichiometry	Heat loss, added CAPEX, and transfer integration

CC BY

JIRRS
Journal International Review of Research Studies

Received: 18/04/ 2026 - **Accepted:** 15/07/2026
Vol: 01.06
DOI: 10.66104/jwmrvy32
Pages: 1-43

Configuration	Strength	Key control variables	Primary scale-up risk
Staged Al in one furnace	Retrofit potential; controllable finishing	CO/CO_2, bath temperature, metal chemistry	Feeder response and bath mixing
Induction furnace	Good mixing and laboratory/pilot control	Power, slag melting, crucible compatibility	Scale and refractory interaction
DC/EAF finishing	High power density; slag control	Arc power, Al rate, residence time	Electrode/arc interaction with exothermic reaction

Note. Representative reactor evidence from Bermúdez et al. (2025), Makhambetov et al. (2026), Mchabe et al. (2026), and Semenov et al. (2024). CAPEX = capital expenditure; DC = direct current; EAF = electric arc furnace.

9. Performance Metrics and a Multi-Criteria Hybrid-Advantage Framework

Hybrid reduction should be evaluated by simultaneous changes in metal recovery, product quality, external energy, direct emissions, slag production, reductant cost, throughput, and process complexity. Product specification is an upstream constraint rather than a downstream score: limits on C, O, Al, inclusions, and alloy chemistry must be fixed before optimizing φAl. A route that lowers direct carbon-derived emissions but doubles slag handling or Al cost is not automatically advantageous. Conversely, a limited Al addition can be justified if it raises overall recovery, shortens furnace time, suppresses carbides, reduces the severity of downstream refining, or reduces external energy enough to offset the added reductant and slag burden.

An unweighted additive "Hybrid Advantage" equation is not physically defensible because recovery, quality, energy, emissions, cost, slag burden, and complexity have different dimensions and depend on the selected system boundary. The framework is therefore better represented as a decision vector, $\Delta H = \{\Delta\text{recovery}, \Delta\text{quality compliance}, \Delta\text{external energy}, \Delta\text{direct } CO_2, \Delta\text{Al cost}, \Delta\text{slag burden}, \Delta\text{complexity}\}$. A scalar score should be calculated only when the direction of benefit, normalization method, weights, and uncertainty are explicitly declared. For process design, φAl remains the main adjustable allocation variable, and the practical optimization problem is to identify the minimum Al share that satisfies recovery and product-quality constraints while meeting energy, economic, and environmental targets.

CC BY

JIRRS
Journal International Review of Research Studies

Received: **18**/04/ 2026 - **Accepted:** 15/07/2026
Vol: 01.06
DOI: 10.66104/jwmrvy32
Pages: 1-43

Table 8 proposes a minimum reporting set. Including oxygen-allocation and reducing-equivalent metrics, together with their calculation basis, would improve comparability between studies that currently report only grams of reductant, wt.% additive, or nominal stoichiometric ratios.

Table 8. *Recommended minimum reporting metrics for hybrid reduction studies.*

Metric	Definition/measurement	Why it is required
φAl and φC	Oxygen share assigned to each reductant; state nominal or balance-derived basis	Compares hybridization across feeds without hiding unreacted reductant
λR	Total supplied oxygen-removal capacity / reducible oxygen; state gas endpoint assumption	Separates allocation from total reductant excess
Recovery and metallization	Metal recovered and oxide converted	Separates chemical conversion from physical metal yield
Specific energy	kWh or MJ per tonne of specification-compliant product; optionally also per tonne feed	Quantifies whether aluminothermic heat actually avoids external energy
Gas intensity	kg or standardized Nm^3 of net CO and CO_2 per tonne product	Captures the direct gas burden
Slag intensity	kg dry slag per tonne product plus Al_2O_3 fraction	Captures the condensed oxygen and separation burden
Product C, Al, and O	Final chemistry, inclusions, and relevant phase fractions	Tests whether hybridization meets the product specification
Residence time/throughput	Time at temperature and mass-processing rate	Essential for scale-up and productivity comparisons

Note. Framework developed in this review and aligned with the reporting patterns in Mchabe et al. (2026), Wiszniewski et al. (2025), and Zhu et al. (2024).

10. Sustainability, Decarbonization, and Techno-Economic Boundaries

Partial substitution of carbon decreases the direct conversion of reductant carbon to CO/CO_2, but direct emissions are only one component of environmental performance. Aluminum production is electricity-intensive and can carry substantial upstream burdens. Life-cycle assessment (LCA) studies of primary and secondary aluminum show that electricity source, recycled content, and dross-recovery route strongly affect the burden assigned to Al when it is used as a reductant (Dardor et al., 2025; Du et al., 2026; Zhang et al., 2023; Zhu & Jin, 2021; Zhu et al., 2020). A decrease in direct furnace CO_2 therefore does not necessarily produce a decrease in cradle-to-gate or cradle-to-product greenhouse-gas emissions.

CC BY

JIRRS
Journal International Review of Research Studies

Received: 18/04/ 2026 - **Accepted:** 15/07/2026
Vol: 01.06
DOI: 10.66104/jwmrvy32
Pages: 1-43

The silicon case makes this boundary explicit. Aluminothermic production can avoid part of the direct carbon footprint of conventional carbothermy, but the life-cycle benefit depends on industrial symbiosis, the source of Al, and the fate or valorization of the alumina-rich slag (Pastor-Vallés et al., 2025; Zhu et al., 2024). A hybrid silicon route could outperform full aluminothermy only under a defined system boundary in which carbon performs the fraction of reduction with the lower system-level burden and low-carbon or secondary Al is reserved for the most difficult finishing step. That proposition should be tested by scenario analysis rather than assumed from direct-emission savings alone.

Economically, a hybrid route becomes plausible when the marginal value created by Al is measurable: higher metal recovery, shorter furnace time, lower external power demand, avoidance of downstream decarburization, or access to a higher-value low-carbon product. It becomes unattractive when Al is consumed by gangue, when alumina-rich slag requires costly fluxing or disposal, or when the product tolerates carbon and the existing carbon-based furnace already operates efficiently. Secondary aluminum streams can change this balance, but their oxide, salt, and impurity contents must be included in both metallurgical accounting and life-cycle inventories (Pereira, 2025; Pereira, 2026b; Pereira, 2026c).

A robust techno-economic analysis (TEA) should therefore report reductant prices and consumption, power and fuel, throughput, furnace campaign effects, slag handling and disposal or valorization, product-price premium, and downstream refining requirements. The economically relevant comparator should be defined as a complete reference route, for example “carbothermy + decarburization/refining” versus “hybrid reduction + reduced refining” versus an aluminothermic route, rather than comparing only the primary reduction steps. LCA should use a functional unit such as one tonne of specification-compliant metal or alloy rather than one tonne of treated feed, because quality losses and metal entrainment can otherwise bias route comparisons. System boundaries, allocation rules for secondary Al, credits for recovered by-products, primary/low-carbon-primary/secondary Al scenarios, and sensitivity to electricity mix should be stated explicitly.

CC BY

JIRRS
Journal International Review of Research Studies

Received: **18**/04/ 2026 - **Accepted:** 15/07/2026
Vol: 01.06
DOI: 10.66104/jwmrvy32
Pages: 1-43

11. Cross-System Evidence and Transferability Boundaries

11.1 Manganese and chromium: staged rationale with limited direct validation

Manganese provides the clearest staged-processing analogue, but not yet the clearest direct C–Al validation. CO/CO_2 pre-reduction has a strong mechanistic foundation, including rate analysis and the effects of moisture and water–gas shift chemistry (Larssen et al., 2021a; Larssen et al., 2021b; Larssen & Tangstad, 2022). Aluminothermic reduction of MnO-bearing slags and kinetic studies of Mn oxides establish a credible finishing chemistry (Kudyba et al., 2021; Salas Avilés et al., 2023). The 200 kW DC-furnace study of aluminothermic smelting after hydrogen pre-reduction demonstrates scale-relevant stage integration, but because the first-stage reductant was H_2 rather than C/CO, it is an architecture analogue and does not close the evidence gap for direct carbothermic–aluminothermic sequencing (Mchabe et al., 2026). Chromium presents a similarly strong rationale where carbide formation is undesirable, although chromite mineralogy and the stability of Cr-bearing oxides narrow the feasible operating window (Carter et al., 2026; Güney et al., 2023).

11.2 Titanium, vanadium, niobium, molybdenum, and tungsten

Titanium systems illustrate the contamination trade-off particularly clearly. Carbothermic processing of ilmenite can generate carbide-bearing products, while aluminothermy readily forms Ti-containing alloys but requires control of residual Al and slag chemistry (Choi et al., 2020; Subasinghe & Ratnayake, 2021; Subasinghe & Ratnayake, 2025; Yang et al., 2022; You et al., 2024). Vanadium and niobium studies demonstrate the value of high-temperature metallothermy when terminal oxygen removal is difficult, but they do not by themselves establish a hybrid C–Al optimum; recent work instead defines relevant thermodynamic, viscosity, and recovery constraints (Godoy et al., 2024; Jain & Awasthi, 2025; Xin et al., 2022; Zhang et al., 2025). Mo/W systems likewise highlight carbide formation, reaction heat, and the potential value of reserving Al for final deoxidation, but the staged hybrid proposition remains a hypothesis that requires direct testing (Bao et al., 2026; Makhambetov et al., 2026; Sheybani et al., 2020; Wang et al., 2025).

CC BY

JIRRS
Journal International Review of Research Studies

Received: 18/04/ 2026 - **Accepted:** 15/07/2026
Vol: 01.06
DOI: 10.66104/jwmrvy32
Pages: 1-43

11.3 Silicon and secondary resources

Silicon is a useful decarbonization benchmark because the conventional route is mature and carbon-intensive. Pilot-scale aluminothermy demonstrates technical feasibility, while LCA shows that the origin of Al and the fate of alumina-rich slag determine whether direct-emission savings persist at the system level (Pastor-Vallés et al., 2025; Zhu et al., 2024). By contrast, secondary resources—including steel slags, battery black mass, mill scale, aluminum dross, and complex residues—provide some of the strongest direct motivations for hybridization because one stream can supply Al while another supplies reducible oxides and carbon may already be present or deliberately added. Direct Al–C reduction roasting and dross–graphite systems show this coupling more explicitly, although impurity redistribution and phase partitioning become central constraints (Bugdayci et al., 2020; Klemettinen et al., 2024; Ma et al., 2022; Nababan et al., 2024a; Nababan et al., 2024b; Wongsawan et al., 2022).

12. Scale-Up, Operating Map, and Research Priorities

12.1 Scale-up constraints

Scale-up changes the balance between reaction heat and heat loss, gas evolution and permeability, Al addition rate and local reaction intensity, and droplet settling and available residence time. Surface-area-to-volume ratio decreases with scale and can improve thermal efficiency, but larger vessels also create longer transport distances, stronger mixing heterogeneity, and greater consequences of local Al overfeeding. A laboratory optimum φAl may therefore be unsafe or ineffective at pilot scale unless Al addition rate, charge stratification, bath circulation, and pressure-relief capacity are scaled deliberately.

The most important scale-up variables are hot-feed temperature, net gas-generation rate, pressure relief, Al feed rate, reaction-front velocity, slag liquidus and viscosity, droplet-size distribution, metal-settling time, bath mixing, and refractory interaction. Pilot aluminothermic silicon production and the 200 kW manganese campaign provide valuable scale-relevant anchors, but the manganese campaign is an $H_2 \rightarrow$Al architecture analogue rather than a direct C→Al demonstration,

CC BY

JIRRS
Journal International Review of Research Studies

Received: **18**/04/ 2026 - **Accepted:** 15/07/2026
Vol: 01.06
DOI: 10.66104/jwmrvy32
Pages: 1-43

and equivalent data remain scarce for most other oxide systems (Mchabe et al., 2026; Zhu et al., 2024). Numerical models of thermite propagation and furnace heating should therefore be coupled with phase-equilibrium, gas-flow, and slag-flow models before extrapolating laboratory φAl optima to industrial vessels (Abdelal, 2026; Semenov et al., 2024). Classical slag–metal thermochemical and transport principles remain essential when translating these variables to larger vessels (Turkdogan, 1996).

12.2 Process-safety envelope for hybrid C–Al scale-up

Process safety must be treated as an independent scale-up domain because hybrid C–Al systems can combine fine Al powders, combustible carbonaceous solids, strongly exothermic thermite-type reactions, rapid CO/CO_2 evolution, splashing, pressure transients, localized refractory overheating, and metal/slag ejection. Pilot design should therefore specify Al-powder storage and transfer controls, ignition-source exclusion, dust-explosion assessment, continuous CO monitoring and off-gas management, pressure-relief capacity, controlled and interlocked Al feeding, emergency feed interruption, thermal monitoring of the refractory/vessel shell, and operating limits for local temperature rise and gas-generation rate. HAZOP and/or FMEA should be completed before scale-up, with credible deviations including Al overfeed, loss of mixing, blocked off-gas, delayed ignition, water ingress, refractory hot spots, and uncontrolled reaction-front propagation. A laboratory optimum in φAl should not be transferred to pilot scale unless it also lies within this defined safety envelope.

12.3 O–T–K–C–S–Q–E operating map

Figure 7 condenses the review into the author-developed O–T–K–C–S–Q–E conceptual decision framework: Oxygen allocation defines φAl and φC; Thermal coupling tests whether Al heat is usefully captured; Kinetics identifies the controlling pathway; Carbon control checks carburization and carbides; Slag and separation determine whether chemically reduced metal is physically recovered; Quality verifies C, Al, O, and inclusion specifications; and Economics/environment determine whether the route remains advantageous at the selected scale and system boundary. The

CC BY

JIRRS
Journal International Review of Research Studies

Received: **18**/04/ 2026 - **Accepted:** 15/07/2026
Vol: 01.06
DOI: 10.66104/jwmrvy32
Pages: 1-43

framework has not yet been prospectively validated as a quantitative process-selection, scoring, or technology-readiness tool. A negative result at a gate should also be interpreted in two distinct ways: technical failure, when the route demonstrably cannot satisfy the criterion, and evidence insufficiency, when available data are inadequate to justify scale-up or a positive decision. This distinction prevents an evidence gap from being misread as proof of technical infeasibility.

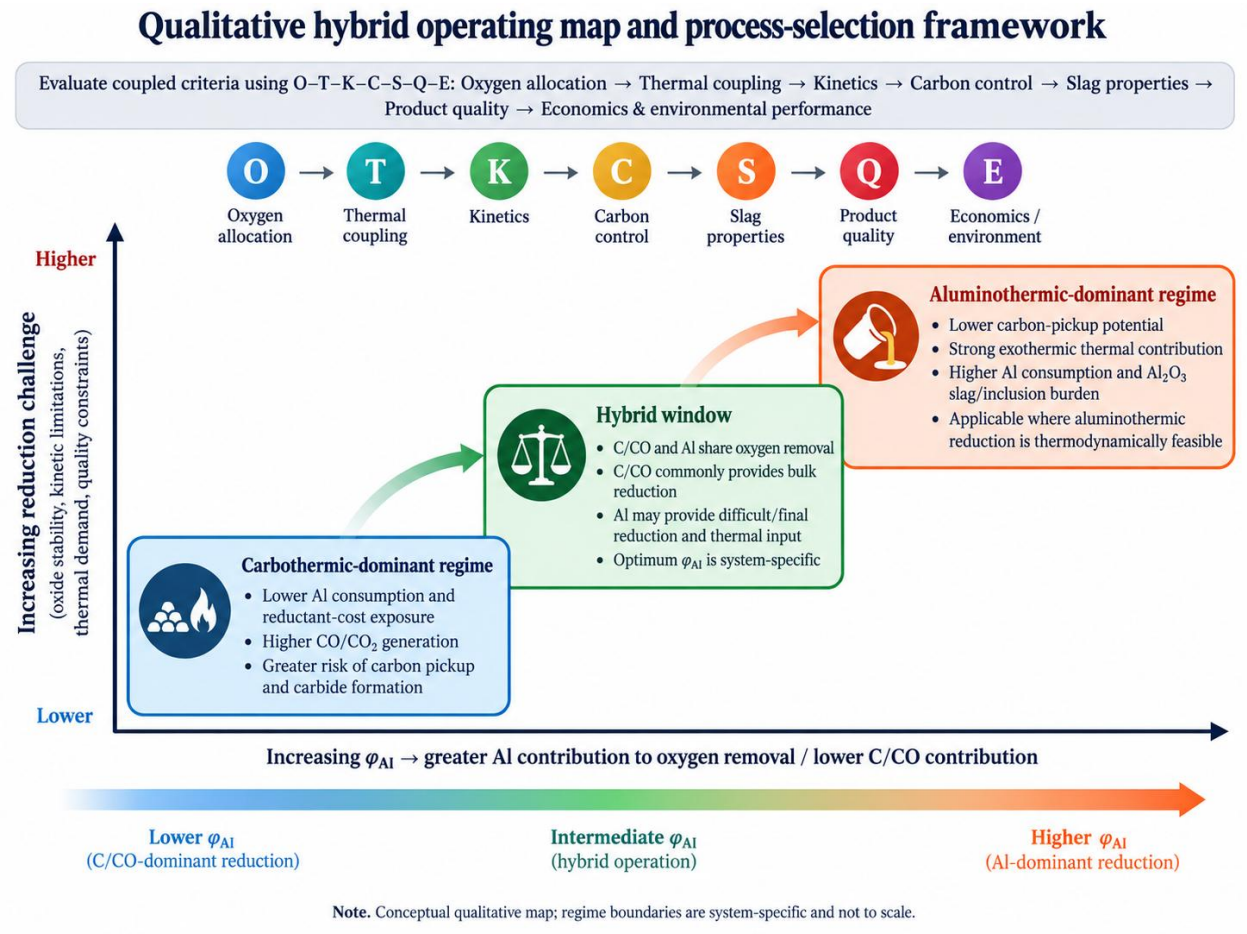

Figure 7. *Hybrid operating map and O–T–K–C–S–Q–E process-selection framework.*

Note. Author-developed conceptual framework synthesized in this review from the evidence in Sections 4–11; it is proposed for prospective testing and is not a validated quantitative scoring or technology-readiness system.

CC BY

JIRRS Journal International Review of Research Studies

Received: **18**/04/ 2026 - **Accepted:** 15/07/2026
Vol: 01.06
DOI: 10.66104/jwmrvy32
Pages: 1-43

12.4 Research priorities

The first research priority is standardization. Hybrid studies should report φAl, φC, λR, the nominal or balance-derived basis of those metrics, direct gas generation, slag intensity, and final C/Al/O chemistry. The second is factorial experimentation that varies carbon and aluminum independently rather than comparing only pure-C and pure-Al endpoints. Such designs can determine whether an interaction is genuinely synergistic, merely additive, or antagonistic. The third is time-resolved characterization: off-gas, temperature, phase evolution, and droplet coalescence should be measured during reduction rather than only after quenching.

The fourth priority is scale-relevant slag and separation testing. Many studies optimize reduction degree but do not quantify viscosity, droplet-size distribution, entrained metal, or settling time. The fifth is dynamic Al feeding using reactor-calibrated off-gas indicators such as $CO/(CO + CO_2)$ together with bath temperature and metal/slag chemistry rather than relying on a universal gas-ratio trigger. The sixth is process-safety validation, including ignition control, dust hazards, pressure relief, feed interlocks, refractory thermal loading, and HAZOP/FMEA before pilot operation. The seventh is coupled TEA–LCA using specification-compliant metal as the functional product and scenario-dependent aluminum footprints. Future work should distinguish primary Al, low-carbon primary Al, and secondary Al reductants because circular Al can improve economics and life-cycle performance while simultaneously introducing oxide, salt, or impurity penalties.

Table 9 summarizes the principal knowledge gaps and the evidence needed to close them. The central gap is not the absence of plausible mechanisms, but the shortage of experiments and pilot campaigns that quantify oxygen allocation, transient heat release, slag separation, and product quality in the same C–Al system.

Table 9. *Research gaps, required evidence, and scale-up relevance.*

Gap	Why current evidence is insufficient	Priority experiment/model	Scale-up value
No common hybridization metric	Reductant additions cannot be compared across feeds	Report φAl, φC, and λR	Enables transferable design maps

CC BY

JIRRS Journal International Review of Research Studies

Received: **18**/04/ 2026 - **Accepted:** 15/07/2026
Vol: 01.06
DOI: 10.66104/jwmrvy32
Pages: 1-43

Gap	Why current evidence is insufficient	Priority experiment/model	Scale-up value
Synergy often asserted, not demonstrated	Endpoint recovery cannot separate thermal and chemical effects	Factorial C × Al × T design with single-reductant controls	Prevents unjustified Al addition
Limited transient data	Mechanism changes during heating/melting	Off-gas + temperature + in situ/quenched phase tracking	Supports staged control
Slag/separation underreported	High reduction may coexist with entrainment loss	Viscosity, droplet size, settling, chemical vs physical loss	Predicts true metal recovery
Few pilot demonstrations	Lab heat loss and mixing are not representative	Pilot campaigns with closed mass/energy balances and declared feed rate/power	Defines a scale-relevant operating envelope
LCA often uses generic Al	Al footprint is scenario-dependent	Primary, low-carbon primary, and secondary Al scenarios	Tests real decarbonization benefit

Note. Critical synthesis of current evidence from Abdelal (2026), Mchabe et al. (2026), Pastor-Vallés et al. (2025), Pereira (2026a), Wiszniewski et al. (2025), and Zhu et al. (2024).

13. Conclusions

Hybrid carbothermic–aluminothermic reduction should be treated as an oxygen-allocation and process-integration problem rather than as the mere simultaneous presence of two reductants. The defining design variable is the fraction of reducible oxygen deliberately assigned to aluminum, φAl, while carbon/CO is retained for the fraction that can be removed economically and without unacceptable product contamination. This framing creates a continuous design space between pure carbothermy and pure aluminothermy, but φAl is meaningful only when its nominal or measured mass-balance basis is stated.

The most credible hybrid strategy is to use aluminum selectively rather than indiscriminately. Carbon can perform low-cost bulk reduction, while Al can be reserved for difficult terminal oxygen removal, useful thermal intensification, or product-quality finishing. The rationale is strongest when conventional carbothermy is constrained by carbon pickup, carbide formation, slow terminal kinetics, or excessive external energy, and when full aluminothermy would impose an unacceptable reductant cost, slag burden, residual-Al risk, or upstream environmental footprint. Direct simultaneous hybrid evidence exists in several secondary-resource and co-reduction

CC BY

JIRRS
Journal International Review of Research Studies

Received: **18**/04/ 2026 - **Accepted:** 15/07/2026
Vol: 01.06
DOI: 10.66104/jwmrvy32
Pages: 1-43

systems, whereas direct pilot-scale C/CO → Al sequential validation remains a major evidence gap.

Thermodynamic feasibility alone is insufficient. Useful aluminothermic heat must be captured rather than lost, carbon and aluminum contamination must both remain within specification, and the resulting slag must permit droplet coalescence and metal recovery. A process that improves chemical reduction but increases physical metal loss, inclusion burden, refractory demand, or slag-handling cost has not demonstrated a net hybrid advantage.

The author-developed O–T–K–C–S–Q–E framework provides a conceptual sequence for future design: allocate oxygen, quantify thermal coupling, identify rate control, manage carbon, engineer slag and separation, verify product quality, and then test economics, environmental performance, and process safety at scale. It has not yet been validated as a quantitative scoring, process-selection, or technology-readiness tool. Future progress depends on standardized oxygen-allocation metrics, factorial C × Al experiments with single-reductant controls, transient measurements, direct C/CO → Al pilot campaigns, closed mass/energy balances, process-safety analysis, and scenario-specific TEA–LCA. The industrial decision is therefore not simply “carbon or aluminum?” but “what is the minimum aluminum share that delivers the required recovery, product quality, energy performance, and decarbonization outcome without transferring the burden to slag, upstream Al production, downstream refining, safety risk, or process complexity?”

Declarations

Funding

This review received no specific external funding.

Conflict of Interest

The author declares no conflict of interest.

Data Availability

No new experimental datasets were generated. All quantitative values discussed in the review are traceable to the cited literature.

Author Contributions

CC BY

JIRRS
Journal International Review of Research Studies

Received: 18/04/ 2026 - **Accepted:** 15/07/2026
Vol: 01.06
DOI: 10.66104/jwmrvy32
Pages: 1-43

Conceptualization, critical analysis, literature synthesis, visualization, and manuscript preparation by the author.

References

Abdelal, G. (2026). A zero-tuning DEM-to-continuum framework for thermite front propagation: Contact-resistance conductivity and diffusion-limited kinetics, implemented through an AI-agent workflow. *Applied Sciences*, *16*(16), 8145. https://doi.org/10.3390/app16168145

Amon, A., Moore, E. E., Henderson, H. B., Shittu, J., Kunz, M., Kastamo, S., Huotari, N., Loukus, A., Ott, R., Weiss, D., & McCall, S. K. (2024). Aluminothermic reduction of CeO_2: Mechanism of an economical route to aluminum–cerium alloys. *Materials Horizons*, *11*(10), 2382–2387. https://doi.org/10.1039/D4MH00087K

An, H., Jiang, X., Ji, H., Zhang, Z., He, L., Zheng, H., Gao, Q., & Shen, F. (2023). Fundamentals of reduction of $CaO{\cdot}Fe_2O_3$ in CO/CO_2 gas at 1000 °C. *Ironmaking & Steelmaking*, *50*(6), 621–629. https://doi.org/10.1080/03019233.2022.2140255

Bao, K., Ma, Y., Tang, J., & Liu, W. (2026). In situ TEM study of WO_3 structural and phase evolution in carbothermal reduction. *Materials Research Letters*, *14*(2), 169–175. https://doi.org/10.1080/21663831.2025.2611734

Bermúdez, A., Crego, O., Ferrín, J. L., García, B., Gómez, D., Martínez, I., Pérez-Pérez, L. J., & Salgado, P. (2025). Multiphysics simulation of slag melting in an induction furnace for sustainable silicon production. *Applied Mathematical Modelling*, *145*, 116107. https://doi.org/10.1016/j.apm.2025.116107

Bugdayci, M., Deniz, G., Ziyreker, C., Turan, A., & Oncel, L. (2020). Thermodynamic modeling and production of FeCo alloy from mill scale through metallothermic reduction. *Engineering Science and Technology, an International Journal*, *23*(5), 1259–1265. https://doi.org/10.1016/j.jestch.2020.03.003

Cai, T., Zhang, Y., Zheng, S., & Zhang, Y. (2026). Reaction pathway of the CaO- and $CaCl_2$-assisted aluminothermic reduction of TiO_2 for the precise fabrication of Ti_2O. *Metallurgical and Materials Transactions B*, *57*(3), 1538–1549. https://doi.org/10.1007/s11663-025-03937-6

Carter, D., Coumans, J. P., Zagrtdenov, N., Duguay, D., & Paktunc, D. (2026). Comparative performance of bio-carbon and petroleum coke as reductants in $CaCl_2$-assisted direct reduction of chromite. *Materials*, *19*(18), 3840. https://doi.org/10.3390/ma19183840

Chen, L., Yang, J., Yang, Y., Zhang, Y., & Wang, Z. (2022). Thermodynamics, kinetics and mechanism analysis of aluminothermic reduction for preparing Al–Zr alloy. *Materials Today Communications*, *31*, 103714. https://doi.org/10.1016/j.mtcomm.2022.103714

CC BY

JIRRS
Journal International Review of Research Studies

Received: 18/04/ 2026 - **Accepted:** 15/07/2026
Vol: 01.06
DOI: 10.66104/jwmrvy32
Pages: 1-43

Cheng, C., Wang, X.-Y., Zhang, T.-A., Dou, Z.-H., Song, K.-X., Wang, M.-X., Feng, Y.-S., Huang, T., Liu, H.-T., Li, X.-H., & Li, K. (2024). Metal-slag separation strengthening through in situ slagging during CuW composite preparation by metallothermic reduction. *Rare Metals*, *43*, 6113–6121. https://doi.org/10.1007/s12598-024-02820-8

Choi, J.-H., Chang, H., Ryu, T., Nam, C.-W., & Kim, B.-S. (2020). Investigating the aluminothermic process for producing ferrotitanium alloy from ilmenite concentrate. *Metals*, *10*(11), 1493. https://doi.org/10.3390/met10111493

Coetsee, T., & De Bruin, F. (2025). Sodium oxide-fluxed aluminothermic reduction of manganese ore with synergistic effects of C and Si reductants: SEM study and phase stability calculations. *Reactions*, *6*(3), 40. https://doi.org/10.3390/reactions6030040

Coetsee, T., & De Bruin, F. (2026). Sodium-oxide fluxed slag design, phase chemistry and thermochemistry calculations for aluminum recycling from aluminothermic reduction of manganese ore. *Crystals*, *16*(6), 401. https://doi.org/10.3390/cryst16060401

Dardor, D., Flórez-Orrego, D., Domingos, M. E. R., Germanier, R., Margni, M., & Maréchal, F. (2025). Towards carbon-negative primary aluminium production: Integrating biomass resources and renewable electricity. *Journal of Cleaner Production*, *534*, 146994. https://doi.org/10.1016/j.jclepro.2025.146994

de Souza, K. M., & de Lemos, M. J. S. (2021). Detailed numerical modeling and simulation of Fe_2O_3–Al thermite reaction. *Propellants, Explosives, Pyrotechnics*, *46*(5), 806–824. https://doi.org/10.1002/prep.202000290

de Souza, K. M., de Lemos, M. J. S., Ribeiro, R. R., Martins, P. G. C., & Gouvêa, L. H. (2024). Experimental and numerical investigation of the effect of alumina on thermite reaction propagation for thermal plug and abandonment of oil wells. *International Journal of Heat and Mass Transfer*, *224*, 125327. https://doi.org/10.1016/j.ijheatmasstransfer.2024.125327

Du, H., Chen, Y., Wang, Y., Wang, H., Guo, X., Zhang, Z., Li, H., Xing, P., & Zhuang, Y. (2025). Thermodynamic mechanism of metallurgical-grade silicon preparation from silica fume by carbothermal reduction. *Journal of Cleaner Production*, *529*, 146817. https://doi.org/10.1016/j.jclepro.2025.146817

Du, Y., Xie, M., Zhao, M., Liu, Y., Liu, Z., & Li, B. (2026). Overview of decarbonization exploration in China's non-ferrous metal industry: A study of the aluminum industry based on life cycle assessment. *Process Safety and Environmental Protection*, *210*, 108716. https://doi.org/10.1016/j.psep.2026.108716

Ellingham, H. J. T. (1944). Reducibility of oxides and sulphides in metallurgical processes. Journal of the Society of Chemical Industry, 63, 125–133.

JIRRS
Journal International Review of Research Studies

Received: 18/04/ 2026 - **Accepted:** 15/07/2026
Vol: 01.06
DOI: 10.66104/jwmrvy32
Pages: 1-43

Feldhagen, H. G., Oliveira, R. P. de, Patrocínio Júnior, C., Pereira, A. C., Souza, J. B. C. de, & Nascimento Júnior, R. da C. (2016). Ensaios mecânicos em aglomerados autorredutores de concentrado de níquel (Mechanical testing of self-reducing agglomerates from nickel concentrate). In *Proceedings of the 46th Reduction/17th Iron Ore/4th Agglomeration Seminar*, 588–593. https://doi.org/10.5151/2594-357X-28003

Feng, C., Gao, L.-H., Tang, J., Liu, Z.-G., & Chu, M.-S. (2020). Effects of MgO/Al_2O_3 ratio on viscous behaviors and structures of MgO–Al_2O_3–TiO_2–CaO–SiO_2 slag systems with high TiO_2 content and low CaO/SiO_2 ratio. *Transactions of Nonferrous Metals Society of China*, *30*, 800–811. https://doi.org/10.1016/S1003-6326(20)65255-4

Godoy, V. E. de, Bagatini, M. C., Galery, R., Netto, D. G., Montenegro, L. C. M., & Caixeta, D. E. (2024). Increase of niobium metallurgical recovery on aluminothermic process. *In 53rd Seminar on Steelmaking, Casting and Non-Ferrous Metallurgy (pp. 80–90).* https://doi.org/10.5151/2594-5300-40547

Güney, H., Güner, Ö., Boncuk, F. F., Kan, S., Benzeşik, K., & Yücel, O. (2023). A decarbonization approach for FeCr production. *Journal of Sustainable Metallurgy*, *9*(1), 216–229. https://doi.org/10.1007/s40831-022-00632-7

He, M., Wang, N., Hou, Q., Chen, M., & Yu, H. (2020). Coalescence and sedimentation of liquid iron droplets during smelting reduction of converter slag with mechanical stirring. *Powder Technology*, *362*, 550–558. https://doi.org/10.1016/j.powtec.2019.12.020

Holappa, L., & Nurmi, S. (2025). Thermodynamic constraints and prospects for intensified steel deoxidation. *Steel Research International*, *96*(8), 2400556. https://doi.org/10.1002/srin.202400556

Hoover, H., Bell, R., & Rippy, K. (2024). Emerging technologies for decarbonizing silicon production. *Journal of Sustainable Metallurgy*, *10*, 1921–1932. https://doi.org/10.1007/s40831-024-00913-3

Hu, Z., Wang, J., Xue, Z., Wang, W., Huang, F., & Mei, X. (2025). The carbothermic reduction behaviour of saprolitic laterite nickel ore and the enhancement mechanisms of selective nickel reduction induced by CaO and CaF_2 incorporation. *Journal of Materials Research and Technology*, *38*, 392–405. https://doi.org/10.1016/j.jmrt.2025.07.217

Jain, U., & Awasthi, A. (2025). The use of Al_2O_3 as heat-sink during vanadium extraction by thermite process. *Mineral Processing and Extractive Metallurgy*, *134*(1), 33–42. https://doi.org/10.1177/25726641241312789

Jiang, H., Zhang, T.-A., & Dou, Z.-H. (2026a). Metallurgical thermodynamic design research on the in situ synthesis of Ti–Al–Nb alloys using thermit self-propagating reduction. *Materials*, *19*(9), 1689. https://doi.org/10.3390/ma19091689

CC BY

JIRRS
Journal International Review of Research Studies

Received: 18/04/ 2026 - **Accepted:** 15/07/2026
Vol: 01.06
DOI: 10.66104/jwmrvy32
Pages: 1-43

Jiang, H., Zhang, T.-A., & Dou, Z.-H. (2026b). Preparation of γ-TiAl alloys via self-propagating aluminothermic reduction–slag washing refining coupled with vacuum arc remelting. *Materials*, *19*(8), 1650. https://doi.org/10.3390/ma19081650

Klemettinen, A., Klemettinen, L., Rinne, T., O'Brien, H., Jokilaakso, A., & Serna-Guerrero, R. (2024). Towards integration of Ni-slag cleaning process and lithium-ion battery recycling for an efficient recovery of valuable metals. *Metallurgical and Materials Transactions B*, *55*, 3372–3386. https://doi.org/10.1007/s11663-024-03185-0

Kudyba, A., Akhtar, S., Johansen, I., & Safarian, J. (2021). Aluminothermic reduction of manganese oxide from selected MnO-containing slags. *Materials*, *14*(2), 356. https://doi.org/10.3390/ma14020356

Kumar, P., Tang, K., & Safarian, J. (2026). Inclusions in ultra-low carbon ferromanganese obtained via aluminothermic reduction of different pre-reduced Mn ores. *Metallurgical and Materials Transactions B*, *57*, 2935–2948. https://doi.org/10.1007/s11663-026-04025-z

Lai, C., Jing, B., Tan, J., & Li, Q. (2026). Investigation of iron droplets assembling in molten slag. *Colloids and Surfaces A: Physicochemical and Engineering Aspects*, *735*, 139463. https://doi.org/10.1016/j.colsurfa.2026.139463

Larssen, T. A., & Tangstad, M. (2022). Effect of moisture, hydrogen, and water–gas shift reaction on the prereduction behavior of Comilog and Nchwaning manganese ores. *Metallurgical and Materials Transactions B*, *53*, 2104–2116. https://doi.org/10.1007/s11663-022-02511-8

Larssen, T. A., Senk, D., & Tangstad, M. (2021a). Reaction rate analysis of manganese ore prereduction in CO–CO_2 atmosphere. *Metallurgical and Materials Transactions B*, *52*, 2087–2100. https://doi.org/10.1007/s11663-021-02162-1

Larssen, T. A., Senk, D., & Tangstad, M. (2021b). Reduction of manganese ores in CO–CO_2 atmospheres. *Metallurgical and Materials Transactions B*, *52*, 363–381. https://doi.org/10.1007/s11663-020-02018-0

Lyu, Z., Gu, C., Lyu, Z., Liu, Y., Liu, Q., Wang, B., Gao, F., & Bao, Y. (2026). A multi-scale ICME framework for designing functional aluminosilicate melts in staged deoxidation processes. *Materials & Design*, *266*, 116182. https://doi.org/10.1016/j.matdes.2026.116182

Ma, S., Liu, F., Li, K., Chen, Z., Chen, F., Wang, J., Zhong, S., Wilson, B. P., & Lundström, M. (2022). Separation of Li and Al from spent ternary Li-ion batteries by in-situ aluminum-carbon reduction roasting followed by selective leaching. *Hydrometallurgy*, *213*, 105941. https://doi.org/10.1016/j.hydromet.2022.105941

CC BY

JIRRS
Journal International Review of Research Studies

Received: 18/04/ 2026 - **Accepted:** 15/07/2026
Vol: 01.06
DOI: 10.66104/jwmrvy32
Pages: 1-43

Makhambetov, Y., Akhmetov, A., Smagulov, A., Sadyk, Z., Kabylkanov, S., Saulebek, Z., & Toleukadyr, R. (2026). Smelting of a complex W-, Mo-, and Cr-containing alloy in an induction furnace via metallothermic reduction. *Alloys*, *5*(2), 11. https://doi.org/10.3390/alloys5020011

Marmolejo-Saucedo, J. A., Litvinchev, I., Bizhanov, A., Yaskov, G., & Romanova, T. (2024). Estimating porosity of agglomerated products using optimized sphere packing. *International Journal of Manufacturing, Materials, and Mechanical Engineering*, *13*(1), 1–19. https://doi.org/10.4018/IJMMME.344425

Mchabe, D., Tsebe, S., Mampuru, M., Safarian, J., & Matinde, E. (2026). Smelting–aluminothermic reduction of hydrogen pre-reduced manganese ores in a 200 kW DC arc furnace. *Metals*, *16*(7), 794. https://doi.org/10.3390/met16070794

Mitas, B., Visuri, V. V., & Schenk, J. (2023). Modeling the residence time of metal droplets in slag during BOF steelmaking. *Metallurgical and Materials Transactions B*, *54*, 1938–1953. https://doi.org/10.1007/s11663-023-02808-2

Mukono, T., Reiersen, H. S., Schanche, T. L., Wallin, M., & Tangstad, M. (2022). Prereduction behavior of manganese ores with solid carbon and in CO/CO_2 gas atmosphere. *Metallurgical and Materials Transactions B*, *53*, 3292–3305. https://doi.org/10.1007/s11663-022-02611-5

Nababan, D. C., Mukhlis, R., Durandet, Y., Prentice, L. H., & Rhamdhani, M. A. (2024a). Separation of Li and Co from $LiCoO_2$ cathode material through aluminothermic reduction: Investigation of the thermite reaction. *Metallurgical and Materials Transactions B*, *55*(2), 905–924. https://doi.org/10.1007/s11663-024-03003-7

Nababan, D. C., Mukhlis, R., Durandet, Y., Prentice, L. H., & Rhamdhani, M. A. (2024b). Separation of Li and Co from $LiCoO_2$ cathode material through aluminothermic reduction: Thermodynamic calculations and experimental results. *Metallurgical and Materials Transactions B*, *55*(1), 352–375. https://doi.org/10.1007/s11663-023-02962-7

Nababan, D. C., Nuraeni, B. A., Rhamdani, A. R., Pownceby, M. I., & Rhamdhani, M. A. (2026). Metallothermic reduction using aluminum for metal and alloy production. International Materials Reviews. Advance online publication. https://doi.org/10.1177/09506608261467561

Nuraeni, B. A., Avarmaa, K., Prentice, L. H., Rankin, W. J., & Rhamdhani, M. A. (2022). Carbothermic reduction of $LiCoO_2$ cathode material: Thermodynamic analysis, microstructure and mechanisms. *Sustainable Materials and Technologies*, *34*, e00526. https://doi.org/10.1016/j.susmat.2022.e00526

CC BY

JIRRS
Journal International Review of Research Studies

Received: 18/04/ 2026 - **Accepted:** 15/07/2026
Vol: 01.06
DOI: 10.66104/jwmrvy32
Pages: 1-43

Panteikov, S. P., Bondarenko, Y. I., Romanenko, A. A., & Uzunov, I. I. (2024). Analysis of the processes of manganese step reduction from its dioxide by CO gas and gasification of solid carbon from the position of thermodynamics. *Modern Problems of Metallurgy*, *27*, 141–158. https://doi.org/10.34185/1991-7848.2024.01.10

Pastor-Vallés, E., Abadías Llamas, A., & Pettersen, J. B. (2025). Carbon-neutral silicon via aluminothermic reduction? Exploring industrial symbiosis through life cycle assessment. *ACS Sustainable Chemistry & Engineering*, *13*(36), 14893–14902. https://doi.org/10.1021/acssuschemeng.5c04666

Pereira, A. C. (2025). Aluminum scrap recycling for foundry alloys: Review of technological advances and circular economy challenges. *Revista DCS*, *22*(84), e3867. https://doi.org/10.54899/dcs.v22i84.3867

Pereira, A. C. (2026a). Liquid-metal droplet coalescence in metallurgical slags: A critical review of interfacial phenomena, slag properties, hydrodynamics, kinetics, and metal recovery. *International Journal of Research and Innovation in Social Science*, *10*(7), 15007–15036. https://doi.org/10.47772/IJRISS.2026.100701023

Pereira, A. C. (2026b). Rotary-furnace recycling of aluminum scrap and dross: A critical review of feedstock–flux–furnace interactions, metal recovery, emissions, and circularity. *Journal International Review of Research Studies*, *1*, 1–50.

Pereira, A. C. (2026c). Secondary aluminum dross and salt slag treatment: A critical review of integrated value recovery, risk control, and industrial readiness. *International Journal of Current Science Research and Review*, *9*(8), 4428–4462. https://doi.org/10.5281/zenodo.21898845

Philipson, H. G. R., Wallin, M., & Einarsrud, K. E. (2024a). Aluminothermic reduction kinetics of calcium silicate slag for silicon alloy production. *Metals*, *14*(6), 604. https://doi.org/10.3390/met14060604

Philipson, H. G. R., Wallin, M., & Einarsrud, K. E. (2024b). Investigation of liquid-liquid reaction phenomena of aluminum in calcium silicate slag. *Materials*, *17*(7), 1466. https://doi.org/10.3390/ma17071466

Rhamdani, A. R., Rhamdhani, M. A., Brooks, G. A., Pownceby, M. I., Thaha, Y. N., Abbott, T. B., Grandfield, J. F., & Hartley, C. J. (2026). Aluminothermic reduction of lanthanum oxide. *Metallurgical and Materials Transactions B*, *57*, 3177–3193. https://doi.org/10.1007/s11663-026-04040-0

Salas Avilés, J. A., Flores Valdés, A., Torres Torres, J., Ochoa Palacios, R. M., & Flores Saldívar, A. A. (2023). A kinetic study on the preparation of Al–Mn alloys by aluminothermic reduction of Mn_3O_4 and MnO powders. *Metals*, *13*(9), 1556. https://doi.org/10.3390/met13091556

CC BY

JIRRS
Journal International Review of Research Studies

Received: 18/04/ 2026 - **Accepted:** 15/07/2026
Vol: 01.06
DOI: 10.66104/jwmrvy32
Pages: 1-43

Sarkar, M., Hossain, R., Ghinangju, B. S., Privat, K., Bhattacharyya, S. K., & Sahajwalla, V. (2026). In situ carbothermic reduction of black mass from spent Li-ion, Ni-MH, and alkaline batteries for Ni-based superalloy synthesis. *ACS Applied Materials & Interfaces*, *18*(27), 37617–37627. https://doi.org/10.1021/acsami.5c19451

Semenov, S., Namy, P., Kale, A., & Tsebe, S. (2024). Numerical model of aluminothermic reduction vessel preheating and charge heating with graphite heating rods. *Open Research Europe*, *4*, 253. https://doi.org/10.12688/openreseurope.18586.1

Sheybani, K., Paydar, M. H., Shariat, M. H., & Setoudeh, N. (2020). An investigation on aluminothermic reduction of MoO_3 in domestic microwave oven. *Journal of Mining and Metallurgy, Section B: Metallurgy*, *56*(3), 361–369. https://doi.org/10.2298/JMMB190312025S

Siame, M. C., Ahmed, H. M., Andersson, A., & Sundqvist-Öqvist, L. (2026). Understanding the thermal behavior of black mass during recycling of spent lithium-ion batteries through its individual components. *ACS Sustainable Chemistry & Engineering*, *14*(4), 1952–1963. https://doi.org/10.1021/acssuschemeng.5c10344

Song, J.-X., Guo, T., Ding, W., Yao, M., Yang, L., Zhang, X.-N., Yu, Z.-S., Wu, J.-X., Zhang, J., & Fang, X. (2020). The effect of Al particles size on the thermal behavior and kinetics of Al–MnO_2 thermite system. *Advances in Materials Science and Engineering*, *2020*, 3097404. https://doi.org/10.1155/2020/3097404

Souza, J. B. C. de, Feldhagen, H. G., Pereira, A. C., & Piumatti, R. (2015). Produção de aglomerados autorredutores e/ou pré-reduzidos a partir de concentrado de níquel (Production of self-reducing and/or pre-reduced agglomerates from nickel concentrate). In *Proceedings of the XXVI Encontro Nacional de Tratamento de Minérios e Metalurgia Extrativa*, Poços de Caldas, Brazil.

Su, P., Pistorius, P. C., & Webler, B. A. (2024). Slag-steel reactions in the refining of advanced high-strength steel. *ISIJ International*, *64*(15), 2203–2209. https://doi.org/10.2355/isijinternational.ISIJINT-2024-229

Subasinghe, H. C. S., & Ratnayake, A. S. (2021). Processing of ilmenite into synthetic rutile using ball milling induced sulphurisation and carbothermic reduction. *Minerals Engineering*, *173*, 107197. https://doi.org/10.1016/j.mineng.2021.107197

Subasinghe, H. C. S., & Ratnayake, A. S. (2025). Thermodynamics, phase transformations, and theoretical perspective of roasting kinetics during sulfurization and carbothermic reduction of ilmenite. *Discover Minerals*, *2*, 5. https://doi.org/10.1007/s44346-025-00010-7

Sun, G.-D., Zhang, G.-H., & Yan, B.-J. (2020). Study on the reduction of commercial MoO_3 with carbon black to prepare MoO_2 and Mo_2C nanoparticles. *International Journal of Applied Ceramic Technology*, *17*, 917–931. https://doi.org/10.1111/ijac.13473

CC BY

JIRRS
Journal International Review of Research Studies

Received: 18/04/ 2026 - **Accepted:** 15/07/2026
Vol: 01.06
DOI: 10.66104/jwmrvy32
Pages: 1-43

Sun, Y., Reddy, K. V., Yousefi, E., Verma, M., Moelans, N., Guo, M., & Seveno, D. (2024). Unravelling the evolution of oxides at the aluminum liquid/vapor interface. *Acta Materialia*, *266*, 119707. https://doi.org/10.1016/j.actamat.2024.119707

Tichtchenko, E., Estève, A., & Rossi, C. (2021). Modeling the self-propagation reaction in heterogeneous and dense media: Application to Al/CuO thermite. *Combustion and Flame*, *228*, 173–183. https://doi.org/10.1016/j.combustflame.2021.01.040

Turkdogan, E. T. (1996). Fundamentals of steelmaking. The Institute of Materials.

Wang, A., Dou, Z., Zhang, T., & Han, J. (2024). Inclusion removal process of homogeneous CuCr50 alloy in-situ synthesized by Al-Mg composite strengthening reduction coupling slagging. *Materials*, *17*(14), 3452. https://doi.org/10.3390/ma17143452

Wang, X., Liao, J., Ma, X., & Zhao, B. (2025). Exothermic and slag formation behavior of aluminothermic reduction of Mo and V oxides. *Metals*, *15*(7), 704. https://doi.org/10.3390/met15070704

Wiszniewski, L., Raonic, Z., Nuraeni, B. A., Marschall, I., Satritama, B., Rhamdhani, M. A., & Riesel, S. (2025). Investigation of thermokinetics in carbo- and aluminothermic reduction of synthesized lithium iron phosphate black mass. *Journal of Cleaner Production*, *503*, 145357. https://doi.org/10.1016/j.jclepro.2025.145357

Wongsawan, P., Srichaisiriwech, W., & Kongkarat, S. (2022). Synthesis of ferroalloys via mill scale-dross-graphite interaction: Implication for industrial wastes upcycling. *Metals*, *12*(11), 1909. https://doi.org/10.3390/met12111909

Xin, J., Wang, N., Chen, M., & Chen, C. (2021). Direct alloying of molten steel with vanadium slag as a substitute of ferrovanadium: Self-reduction behavior of vanadium slag briquette with aluminum dross addition. *Metallurgical and Materials Transactions B*, *52*(2), 815–829. https://doi.org/10.1007/s11663-020-02055-9

Xin, J., Wang, N., Chen, M., & Lv, X. (2022). Viscosity and structure evolution of molten vanadium slag during carbothermic reduction process. *Journal of Non-Crystalline Solids*, *595*, 121840. https://doi.org/10.1016/j.jnoncrysol.2022.121840

Xiong, Y., Qiu, D., Li, A., Omran, M., Ren, J., Lu, C., Yao, H., Li, M., Xie, H., & Yu, Y. (2025). A multi-physical field coupling modeling incorporated the non-thermal effect: Carbothermic reduction of $ZnFe_2O_4$ by using microwave heating. *Energy*, *328*, 136623. https://doi.org/10.1016/j.energy.2025.136623

Yang, J., Wang, Y., Peng, J., & Di, Y. (2022). Reaction mechanism and kinetics of ferrotitanium preparation by aluminothermic reduction of $CaTiO_3$. *Materials Today Communications*, *30*, 102995. https://doi.org/10.1016/j.mtcomm.2021.102995

CC BY

JIRRS
Journal International Review of Research Studies

Received: 18/04/ 2026 - **Accepted:** 15/07/2026
Vol: 01.06
DOI: 10.66104/jwmrvy32
Pages: 1-43

You, J., Yang, J., Dong, W., Wang, Y., & Wang, Y. (2024). Preparation of ferrotitanium alloy by aluminothermic reduction of perovskite. *Process Safety and Environmental Protection*, *187*, 305–311. https://doi.org/10.1016/j.psep.2024.04.102

Zhang, Y., Cai, Y., Liu, S., Su, Z., & Jiang, T. (2023). Life cycle assessment of aluminum-silicon alloy production from secondary aluminum in China. *Journal of Cleaner Production*, *392*, 136214. https://doi.org/10.1016/j.jclepro.2023.136214

Zhang, Z., Zhang, Y., Xue, N., Liu, H., Hu, P., & Bo, W. (2025). Study on the novel method for preparing vanadium-aluminum alloy using calcium vanadate in electro-aluminothermic process. *Journal of Alloys and Compounds*, *1039*, 183138. https://doi.org/10.1016/j.jallcom.2025.183138

Zhu, M., Philipson, H., Blandhol, K., Djupvik, V., Engvoll, K., Safarian, J., Tang, K., Görnerup, M., Pastor-Vallés, E., Wallin, M., & Tranell, G. (2024). Pilot-scale aluminothermic production of silicon alloy and alumina-rich slag. *ACS Sustainable Chemistry & Engineering*, *12*(40), 14795–14809. https://doi.org/10.1021/acssuschemeng.4c05326

Zhu, X., & Jin, Q. (2021). Comparison of three emerging dross recovery processes in China's aluminum industry from the perspective of life cycle assessment. *ACS Sustainable Chemistry & Engineering*, *9*(19), 6776–6787. https://doi.org/10.1021/acssuschemeng.1c00960

Zhu, X., Jin, Q., & Ye, Z. (2020). Life cycle environmental and economic assessment of alumina recovery from secondary aluminum dross in China. *Journal of Cleaner Production*, *277*, 123291. https://doi.org/10.1016/j.jclepro.2020.123291

CC BY